Journal of Mathematical Biology manuscript No.
(will be inserted by the editor)

Equilibria and Stability of a Class of Positive Feedback Loops

Mathematical Analysis and its Application to Caspase-Dependent Apoptosis

Fernando López-Caamal · Richard H. Middleton · Heinrich J. Huber

Received: date / Accepted: date

Abstract Positive feedback loops are common regulatory elements in metabolic and protein signalling pathways. The length of such feedback loops determines stability and sensitivity to network perturbations. Here we provide a mathematical analysis of arbitrary length positive feedback loops with protein production and degradation. These loops serve as an abstraction of typical regulation patterns in protein signalling pathways. We first perform a steady state analysis and, independently of the chain length, identify exactly two steady states that represent either biological activity or inactivity. We thereby provide two formulas for the steady state protein concentrations as a function of feedback length, strength of feedback, as well as protein production and degradation rates. Using a control theory approach, analysing the frequency response of the linearisation of the system and exploiting the Small Gain Theorem, we provide conditions for local stability for both steady states. Our results demonstrate that, under some parameter relationships, once a biological meaningful *on steady state* arises, it is stable, while the *off steady state*, where all proteins are inactive, becomes unstable. We apply our results to a three-tier feedback of caspase activation in apoptosis and demonstrate how an

The authors would like to thank Ms. Niamh Connolly and the anonymous reviewers for thoroughly reviewing the manuscript and providing helpful ideas.
F.L.-C. acknowledges that this work was supported by National Biophotonics and Imaging Platform, Ireland, and funded by the Irish Government's Programme for Research in Third Level Institutions, Cycle 4, Ireland EU Structural Funds Programmes 2007-2013.
H. J. H. acknowledges the support by Science Foundation Ireland via grant 08/IN.1/B1949.

F. López-Caamal
Hamilton Institute, NUI Maynooth, Co. Kildare, Ireland.

R.H. Middleton
Centre for Complex Dynamic Systems & Control, The University of Newcastle, Australia.

H.J. Huber
Centre for Systems Medicine, Department of Physiology & Medical Physics, Royal College of Surgeons in Ireland, Dublin, Ireland.
Tel.: + 353 1 402 8538; Fax: + 353 1 402 2447 E-mail: Heinhuber@rcsi.ie

intermediary protein in such a loop may be used as a signal amplifier within the cascade. Our results provide a rigorous mathematical analysis of positive feedback chains of arbitrary length, thereby relating pathway structure and stability.

Keywords Positive feedback · Recursive protein activation · Apoptosis · ODE · Equilibrium points · Local stability

Mathematics Subject Classification (2000) 92B99 · 93C05 · 93D25 · 37N25 · 92C42 · 97M60

1 Introduction

Feedback loops are core pathway motifs in biochemical signal transduction and crucially affect the dynamical behaviour of the proteins and metabolites under study. Positive feedbacks are common motifs that exhibit robust signalling [6], to stabilise signals over a long range [12,17] or to filter out spatial noise [24], whereas negative feedback loops have been implied in generating transient activation pulses and sustained oscillations. In cases where cellular signals have to be tightly regulated or a terminal, irreversible decision has to be reached, feedback loops are of special importance. As such, during induction of the programmed cell death programme (apoptosis), several positive and negative feedback loops prevent accidental cell death and guarantee that only purposeful apoptosis is robustly executed [23,29,1].

The prevalence of feedback chains in signal transduction and how their length relates to the specific biological contexts has previously been investigated. Originally, positive feedback loops consisting of three or more nodes were less frequently noticed in protein interaction networks of E. Coli than randomised networks. As a consequence, long positive feedback loops were denoted as anti-motifs [2]. However, a more recent study suggested that long positive feedback cascades may be favoured when a higher degree of sensitivity to environmental cues is needed [25].

In this paper, we analyse a circular protein activation mechanism with an arbitrary number of intermediate activation steps and identical reaction topology for each step. We show that this reaction network presents only two steady states and derive closed-form analytic expressions for these steady states in terms of the kinetic parameters. We first characterise the steady states with Theorem 3 in Section 5, giving exact formulas in terms of the kinetic parameters. We then avail of the Small Gain Theorem to obtain sufficient conditions to guarantee local stability of the equilibria. Under some restrictions on the kinetic parameters of the network, these conditions are also necessary. We present these results in Section 6 as Theorems 4 and 5.

To conclude our study, in Section 7 we illustrate how intermediate nodes in positive feedback loops can sense and amplify small fluctuations and illustrate this on the example of the caspase-3/6/8 feedback loop that is present during intrinsic apoptosis.

2 Biological Motivation: Intrinsic, Caspase-dependent Apoptosis

Intrinsic apoptosis is a typical example of a signal transduction process where several positive feedbacks of different chain lengths are present. This process is activated during cellular stress such as after DNA damage caused by irradiation or chemotherapy [14]. Its canonical pathway is depicted in Figure 1A, where it can be seen that the central executioner of cell death, the protease caspase-3, is involved in several positive feedback loops and these feedback loops result in the activation of further molecules of inactive caspase-3.

In one of these loops, caspase-3 feeds back to the protein BID which is further activated by proteolytic cleavage. The presence of more active BID [31] amplifies the activity of the loop given in Figure 1A (panel Ia). In a second loop, active caspase-3 cleaves active caspase-9 to an even more enzymatically active form Figure 1A (panel Ib) [36]. Finally, downstream of caspase-3 activation, further amplification of caspase-3 is mediated by a three tier feedback [7, 18] Figure 1A (panel II) which will be investigated in further detail in Section 7.

All three positive feedback loops show the amplification of caspase-3 activity via chains of different lengths. An abstraction of such loops is depicted in Figure 1B. In this scheme, each network node i (boxes denoted with P^i) is activated by its preceding node, and, after a number of activation steps p, the feedback is assumed to be closed. This feedback chain will be studied in further detail.

For completeness, we note that in Figure 1A additional regulation is provided by the anti-apoptotic protein XIAP which through binding caspase-3 and caspase-9 can attenuate apoptosis (panel IIIa and IIIb). In turn, XIAP gets attenuated by the pro-apoptotic protein Smac (panel IV) [9]. However, we note that due to mutations, several cells fail to express XIAP [27] and, in such cells, the XIAP/Smac branch can be neglected. For these reasons and in order to focus on the role that feedbacks exercise in apoptosis, we further neglect these intricacies.

3 Mathematical Problem Formulation and Methodology

3.1 Representation of the Biochemical Reaction Networks

In the following, we will develop the mathematical model of a sequential activation of cellular proteases such as caspases with an arbitrary number p of activation steps. For this system, we will derive closed-form formulas for the steady states, allowing investigation of the differences between short and long activation loops as depicted in Figure 1B.

The interaction of species in a reaction network is represented by

$$\sum_{i=1}^{n} a_{ij} S_i \xrightarrow{v_j} \sum_{i=1}^{n} b_{ij} S_i, \tag{1}$$

where S_i is the ith species in the jth reaction. In turn, a_{ij} and b_{ij} denote the stoichiometric coefficients of the corresponding species. The temporal dynamics of the concentrations are governed by an ordinary differential equation (ODE) of the form

$$\frac{\mathrm{d}}{\mathrm{d}t}\mathbf{c} = \mathbf{N}\mathbf{v}(\mathbf{c}). \tag{2}$$

Here, $\mathbf{c}(t) : \mathbb{R}_+ \to \mathbb{R}^n$ comprises the trajectories of the species concentrations in (1). The vector $\mathbf{v}(\mathbf{c}(t)) : \mathbb{R}_+ \to \mathbb{R}^m$ is composed of the rates at which the reactants are converted to products. In general, these reaction rates are nonlinear functions of the state $\mathbf{c}(t)$ and modelled, for instance, by the Law of Mass Action. The stoichiometric matrix $\mathbf{N} \in \mathbb{R}^{n\times m}$ relates the reaction rates to changes of the actual concentrations. Its ij^{th} element is defined as

$$N_{ij} = b_{ij} - a_{ij}.$$

The stoichiometric matrix $\mathbf{N}$ will play a major role in the characterisation of the steady states of our autoactivation system. We recall that once a stable equilibrium point is reached, the concentrations of the network will remain at this value for all future time, unless a large external perturbation suddenly modifies the concentration within the network. The equilibrium points will be denoted in the following as $\bar{\mathbf{c}}$ and according to (2) satisfy

$$\mathbf{0} = \mathbf{N}\mathbf{v}(\bar{\mathbf{c}}). \tag{3}$$

Hence, $\mathbf{v}(\bar{\mathbf{c}})$ belongs to the null space of the linear map $\mathbf{N}$. In order to find a closed-form expression for the equilibrium point of (2) as a function of the reaction kinetic parameters, we will make use of this subspace in Sections 4.1 and 5.2.

3.2 Local Stability Analysis of Interconnected Systems

In Section 6 we will analyse the conditions under which the steady states are stable and how the reaction network can toggle its biological state. This stability analysis will be performed on the linearisation of the reaction network in (2), which is given by a set of ODEs of the form

$$\frac{\mathrm{d}}{\mathrm{d}t}\mathbf{e} = \mathbf{A}\mathbf{e} + \mathbf{B}\mathbf{u}, \tag{4a}$$

$$\mathbf{y} = \mathbf{C}\mathbf{e} + \mathbf{D}\mathbf{u}. \tag{4b}$$

In this system, $\mathbf{e}$ represents the species concentrations referred to their equilibrium concentration and is defined by $\mathbf{e} = \mathbf{c} - \bar{\mathbf{c}}$. The functions $\mathbf{u}(t) : \mathbb{R}_+ \to \mathbb{R}^w$ and $\mathbf{y}(t) : \mathbb{R}_+ \to \mathbb{R}^q$ denote the external input and the output of the system, respectively. The matrix $\mathbf{A}$ is the Jacobian of the system, whereas the matrix $\mathbf{B}$ represents how the external inputs comprised in $\mathbf{u}(t)$ interact with the change rate of the species. Likewise, the matrices $\mathbf{C}$ and $\mathbf{D}$ define the output of the system in terms of the state $\mathbf{e}(t)$ and the input $\mathbf{u}(t)$.

For the stability analysis, we will adopt an input-output approach, availing of the so-called *transfer function* of the system (4), which captures the dynamical behaviour of the system when its state is close to the equilibrium. This transfer function represents the relationship between the Laplace transform of the output $\mathbf{Y}(s)$ and the Laplace transform of the input $\mathbf{U}(s)$. When the initial conditions for $\mathbf{e}$ are zero, the transfer function $\mathbf{H}(s)$ relates the input to the output by

$$\mathbf{Y}(s) = \mathbf{H}(s)\mathbf{U}(s). \tag{5}$$

Here $\mathbf{H}(s)$ is given by

$$\mathbf{H}(s) = \mathbf{D} + \mathbf{C}(s\mathbf{I} - \mathbf{A})^{-\mathbf{1}}\mathbf{B}. \tag{6}$$

This formula arises from the Laplace transform of the linear system (4), representing this model in the frequency domain s. This allows us to express (4) as an algebraic relationship that describes the output of the system $\mathbf{Y}(s)$ as a function of the input $\mathbf{U}(s)$. This relationship is explicitly given by the transfer function $\mathbf{H}(s)$ in (6). For further discussion and details on this derivation, we refer to [28].

We say that the system (4) is stable if and only if all the poles of (6) have negative real part (Theorem 4.7 in [30]). The basic notion of input-output stability is that a small input $\mathbf{u}$ will yield a small output $\mathbf{y}$. In order to characterise the input-output properties of the system (4), we require a means to measure the 'size' of a signal. For this purpose, we define the $\mathcal{L}_z$ norm of a signal as

$$||\mathbf{u}||_{\mathcal{L}_z} := \left(\int_0^\infty \left(||\mathbf{u}(t)||_z \right)^z \, \mathrm{d}t \right)^{1/z}, \tag{7}$$

where $||\mathbf{u}(t)||_z$ is the z-norm of $\mathbf{u}$ defined as

$$||\mathbf{u}(t)||_z := \left(\sum_{i=1}^{w} \left(u_i(t) \right)^z \right)^{1/z}.$$

When $||\mathbf{u}||_{\mathcal{L}_z}$ is finite , we say that this signal belongs to the $\mathcal{L}_z$ space. However, the definition in (7) is a bit restrictive, since there are many signals (e.g. a constant function) that do not belong to the $\mathcal{L}_z$ space. To consider a less restrictive space, we consider the time truncation of a signal:

$$\mathbf{u}_\tau(t) := \begin{cases} \mathbf{u}(t) : t < \tau, \\ 0 \quad\;\; : t \geq \tau. \end{cases} \tag{8}$$

If $||\mathbf{u}_\tau||_{\mathcal{L}_z} < \infty \; \forall \, \tau < \infty$, we say that the signal belongs to the Extended $\mathcal{L}_z$ space: $\mathcal{L}_{ze}$.

In the remainder of the paper, we will focus on the $\mathcal{L}_2$ norm of the signals for which a tight bound on the gain γ can be readily computed. This bound is given by the following theorem.

Theorem 1 *Consider the linear time-invariant system in* (4)*, where all the eigenvalues of* $\mathbf{A}$ *have negative real part, and its transfer function* $\mathbf{H}(j\omega) \in \mathbb{C}^{q\times w}$ *is given in* (6)*. Then the* $\boldsymbol{\mathcal{L}_2}$ ***gain*** *of the system is*

$$\gamma := \sup_{\omega\in\mathbb{R}_+} ||\mathbf{H}(j\omega)||_2 = \sup_{\omega\in\mathbb{R}_+} \sqrt{\bar{\lambda}\left(\mathbf{H}^*(j\omega)\mathbf{H}(j\omega)\right)},$$

where $\bar{\lambda}(\mathbf{X})$ *denotes the maximum eigenvalue of* $\mathbf{X}$*.*

The proof of the theorem above can be found in [21]. For a single-input single-output transfer function, i.e. $h(j\omega) \in \mathbb{C}$, its gain γ can, thus, be computed as

$$\gamma := \sup_{\omega\in\mathbb{R}_+} |h(j\omega)| = \sup_{\omega\in\mathbb{R}_+} \sqrt{h^*(j\omega)h(j\omega)}. \tag{9}$$

Once the gain of the system is characterised, the following theorem provides sufficient conditions to determine stability of the feedback connection depicted in Figure 2.

Theorem 2 (Small Gain Theorem) *Consider the interconnected system depicted in Figure 2, where* $\mathbf{H}(s)$ *is stable. Then, the closed-loop system is stable if*

$$||\mathbf{H}(j\omega)|| < 1 \quad \forall \quad \omega \in \mathbb{R}.$$

Here $||\mathbf{H}(j\omega)||$ denotes any induced norm. However, in the rest of the paper we will restrict our attention to the induced $\mathcal{L}_2$ norm characterised in Theorem 1. The proof of this theorem can be found in [30].

We conclude with a remark on the notation to be used. In the following, all superscript indices will be used to denote different variables, instead of an exponent. For example, c_1^2 is used to denote the concentration of the first species type within the second element of the feedback loop. When needed, the operation of exponentiation will be explicitly denoted with round brackets: $c_j^i \times c_j^i = \left(c_j^i\right)^2$. This notation will become useful when the generalised, multiple-tier protein activation is studied. Before studying this generalised system, we will in the next section motivate our ideas to characterise the steady states and the local stability of the system in Figure 1B by analysing a protein autoactivation mechanism ($p = 1$).

4 Equilibrium and Local Stability Analysis of a Protein Autoactivation

In this section we study a simple protein autoactivation. While such a mechanism was previously discussed in a spatiotemporal setup [24], here we will exploit it as a motivating example for our stability analysis. This parameter-independent approach will later be generalised to feedback loops of arbitrary length as depicted in Figure 1B.

Autoactivation is described by the interaction of a protein (P^1) with its activated form (A^1) resulting in two active molecules of A^1. We further consider protein turnover (production and degradation [10]) for P^1 and degradation for A^1. We depict these processes by the following reaction network

$$P^1 + A^1 \xrightarrow{k_1^1} 2A^1,$$
$$A^1 \xrightarrow{k_2^1} 0,$$
$$P^1 \underset{k_{3b}^1}{\overset{k_{3f}^1}{\rightleftharpoons}} 0.$$

In the latter reaction, the subindex 'f' stands for the forward direction of the reaction: $P^1 \xrightarrow{k_{3f}^1} 0$, whereas the subindex '$b$' denotes the backward direction: $0 \xrightarrow{k_{3b}^1} P^1$. We will use this notation in the rest of the paper.

Defining the vector $\mathbf{c}^1 = ([P^1]\ [A^1])^T$ and assuming a mass-action kinetics, the stoichiometric matrix $\mathbf{N}^1$ and the reaction vector $\mathbf{v}^1(\mathbf{c}^1)$ are given by

$$\mathbf{N}^1 = \begin{pmatrix} -1 & 0 & -1 \\ 1 & -1 & 0 \end{pmatrix} \tag{10a}$$
$$\mathbf{v}^1(\mathbf{c}^1) = (k_1^1 c_1^1 c_2^1 \quad k_2^1 c_2^1 \quad k_{3f}^1 c_1^1 - k_{3b}^1)^T, \tag{10b}$$

where the subindex 1 in c_1^1 denotes the inactive protein and the subindex 2 in c_2^1 denotes the active protein. We will keep this notation throughout the rest of the paper. The temporal evolution of the concentrations in $\mathbf{c}^1$ is then governed by (cf. (2))

$$\frac{\mathrm{d}}{\mathrm{d}t}\mathbf{c}^1 = \mathbf{N}^1\mathbf{v}^1(\mathbf{c}^1). \tag{11}$$

4.1 Equilibrium Points

The existence of equilibrium sets (steady states) has been investigated by different approaches. The Chemical Reaction Network Theory (CRNT) by Feinberg, Horn, and Jackson [11], calculates the number of steady states of a chemical reaction network and investigates their local stability. Likewise, in [8], the number of positive steady states is studied by means of the degree theory for general complex reaction networks. However, both approaches fail to provide formulas to calculate equilibrium concentrations of the species, in terms of the kinetic parameters. In this section, we derive closed-form formulas for the steady states of the autoactivation depicted in Figure 1B, when $p = 1$.

We will show that this reaction network has two steady states: a state where the concentrations of all active proteins are zero and a state where the concentrations of all the active proteins are positive. These states will be denoted as the *off steady state* and the *on steady state* throughout the rest of the paper. We further note that the *on steady state* is only biologically meaningful when concentrations of all species have positive values.

In order to determine the equilibria set for this model, we recall that all steady states $\bar{\mathbf{c}}^1$ satisfy

$$\mathbf{N}^1\mathbf{v}^1\left(\bar{\mathbf{c}}^1\right) = \mathbf{0}. \tag{12}$$

We note that to satisfy (12), $\mathbf{v}^1\left(\bar{\mathbf{c}}^1\right)$ must belong to the right null space of $\mathbf{N}^1$. Let the columns of $\mathbf{K}^1 \in \mathbb{R}^{m\times r}$ form a basis for this null space. According to the Rank Nullity Theorem, the number of columns of $\mathbf{K}^1$ is $r = \#\text{col}(\mathbf{N}^1) - \text{rank}\left(\mathbf{N}^1\right)$. Since (12) implies that $\mathbf{v}^1\left(\bar{\mathbf{c}}^1\right) \in \text{Null}(\mathbf{N}^1)$, we can express any element of a vector space as a linear combination of its basis. Hence, there exists a vector $\boldsymbol{\vartheta}^1 \in \mathbb{R}^r$ such that

$$\mathbf{K}^1\boldsymbol{\vartheta}^1 = \mathbf{v}^1\left(\bar{\mathbf{c}}^1\right). \tag{13}$$

In particular, for our case study, we have that $r = 3 - 2 = 1$ and

$$\mathbf{K}^1 = \begin{pmatrix}-1 & -1 & 1\end{pmatrix}^T. \tag{14}$$

From (10b) and (13), we conclude

$$k_1^1\bar{c}_1^1\bar{c}_2^1 = -\vartheta^1, \tag{15a}$$
$$k_2^1\bar{c}_2^1 = -\vartheta^1, \tag{15b}$$
$$k_{3f}^1\bar{c}_1^1 - k_{3b}^1 = \vartheta^1. \tag{15c}$$

To solve this system, we express $\bar{c}_1^1$ and $\bar{c}_2^1$ as a function of ϑ^1:

$$\bar{c}_1^1 = \frac{\vartheta^1 + k_{3b}^1}{k_{3f}^1}, \tag{16a}$$
$$\bar{c}_2^1 = -\frac{\vartheta^1}{k_2^1}. \tag{16b}$$

Substitution of these two expressions in (15a), yields

$$\begin{aligned} -\vartheta^1 &= -\frac{k_1^1}{k_2^1k_{3f}^1}\vartheta^1(\vartheta^1 + k_{3b}^1) \\ 0 &= \vartheta^1\left(\vartheta^1 - \frac{k_2^1k_{3f}^1 - k_1^1k_{3b}^1}{k_1^1}\right). \end{aligned} \tag{17}$$

Finally, by substituting the roots of the polynomial above into (16a) and (16b), we obtain

$$\textbf{Off steady state}: \bar{\mathbf{c}}_{\text{off}}^1 = \begin{pmatrix}\frac{k_{3b}^1}{k_{3f}^1} & 0\end{pmatrix}^T, \tag{18a}$$

$$\textbf{On steady state}: \bar{\mathbf{c}}_{\text{on}}^1 = \begin{pmatrix}\frac{k_2^1}{k_1^1} & \frac{k_{3b}^1}{k_2^1} - \frac{k_{3f}^1}{k_1^1}\end{pmatrix}^T. \tag{18b}$$

It is noteworthy that we can parametrise the solution of the augmented system (15a-15c) by ϑ^1, as shown in (17). Moreover, we note that the dimension

of the null space of $\mathbf{N}^1$ is 1, and, therefore, only one scalar ϑ^1 is required to represent the linear combination that spans the null space Null($\mathbf{N}^1$). We finally note that, since all kinetic constants k_j^1 are positive, the *on steady state* has positive, and therefore biologically meaningful, concentrations whenever $\frac{k_{3b}^1}{k_2^1} > \frac{k_{3f}^1}{k_1^1}$. In the next subsection, we will analyse the local stability of the steady states in (18).

4.2 Local Stability Analysis

Having obtained an analytical expression for the concentrations in equilibrium, we next investigate the stability of both steady states. Several approaches to stability analysis have been described in the literature. In [3] and references therein, they provided the so-called 'secant condition' as a necessary condition to ensure the (diagonal) stability of a reaction network, whose linear dynamical system can be described by circulant matrix. Furthermore, [19] extended the results of [3] to reaction diffusion systems, where they ruled out diffusion driven instability arising from diffusion coefficients of different magnitudes [33]. Despite similarities between the approach of [3] and ours, their system did not account for feedback terms that include products of concentrations $\left(k_1^i c_1^i c_2^{i+1}\right)$ arising from a mass action description of reaction kinetics of our protein interaction cascade (10b).

Analysing the global stability of a nonlinear system with a locally Lipschitz nonlinearity such as $k_1^1 c_1^1 c_2^1$ can be a difficult task. We therefore investigate the *local stability* of both equilibrium points in (18). For this purpose, we investigate the stability of the system's linearisation, which may be used to conclude the local stability of the studied equilibrium point of the nonlinear system [21]. We present sufficient conditions on the parameters to guarantee the local stability of each equilibrium point in (18). To do so, we will express the linearisation of (11) as the unitary feedback loop depicted in Figure 2. After computing the $\mathcal{L}_2$ gain of the linearisation of (11), we will avail of the Small Gain Theorem (2) to derive local stability conditions. Motivated by this procedure, we will generalise these results to an arbitrary number of activation steps p in Section 6.

The linearisation of (11), with the stoichiometric matrix $\mathbf{N}^1$ and the reaction vector $\mathbf{v}^1\left(\mathbf{c}^1\right)$ in (10), is given by

$$\frac{\mathrm{d}}{\mathrm{d}t}\mathbf{e}^1 = \mathbf{A}^1\mathbf{e}^1, \tag{19}$$

where $\mathbf{e}^1 := \mathbf{c}^1 - \bar{\mathbf{c}}^1$ denotes the species concentrations referred to the steady state $\bar{\mathbf{c}}^1$. Here $\mathbf{A}^1$ is the Jacobian of (11):

$$\frac{\mathrm{d}}{\mathrm{d}\mathbf{c}^1}\mathbf{N}^1\mathbf{v}^1\left(\mathbf{c}^1\right) = \begin{pmatrix} -\mu^1 & 0 \\ \mu^1 - k_{3f}^1 & -k_2^1 \end{pmatrix} + \sigma^1 \begin{pmatrix} 0 & -1 \\ 0 & 1 \end{pmatrix} = \mathbf{A}^{11} + \mathbf{B}^1\mathbf{C}. \tag{20}$$

Additionally, we have defined

$$\sigma^{1} := k_1^{1}\bar{c}_1^{1} \tag{21a}$$
$$\mu^{1} := k_1^{1}\bar{c}_2^{1} + k_{3f}^{1}, \tag{21b}$$

and

$$\mathbf{B}^{1} := \sigma^{1}\begin{pmatrix} -1 \\ 1 \end{pmatrix} \tag{22a}$$
$$\mathbf{C} := \begin{pmatrix} 0 & 1 \end{pmatrix}. \tag{22b}$$

By letting $u^{1} = y^{1}$ and considering the definitions above, we can rewrite (19) as

$$\frac{\mathrm{d}}{\mathrm{d}t}\mathbf{e}^{1} = \mathbf{A}^{11}\mathbf{e}^{1} + \mathbf{B}^{1}u^{1}, \tag{23a}$$
$$y^{1} = \mathbf{C}\mathbf{e}^{1}. \tag{23b}$$

The transfer function of the system (23), as defined in (6), is given by

$$h^{1}(s) = \sigma^{1}\frac{s + k_{3f}^{1}}{(s+\mu^{1})(s+k_2^{1})}. \tag{24}$$

We note that if $\mu^{1} > 0$, then the transfer system above is stable. Moreover, we note that given the definition of μ^{1} in (21) and the positivity of parameters, μ^{1} is always positive.

Furthermore, from (9), the $\mathcal{L}_2$ gain of the transfer function above is given by

$$\gamma^{1} = |\sigma^{1}| \sup_{\omega\in\mathbb{R}} \sqrt{\frac{\omega^2 + \left(k_{3f}^{1}\right)^2}{\left[\omega^2 + \left(\mu^{1}\right)^2\right]\left[\omega^2 + \left(k_2^{1}\right)^2\right]}}. \tag{25}$$

Now, we note that the square root function is a monotonically increasing function of its argument. Hence, the supremum of the square root in (25) is given by the square root of the supremum of the argument. Therefore

$$\gamma^{1} = |\sigma^{1}| \sqrt{\sup_{\omega\in\mathbb{R}} \frac{\omega^2 + \left(k_{3f}^{1}\right)^2}{\left[\omega^2 + \left(\mu^{1}\right)^2\right]\left[\omega^2 + \left(k_2^{1}\right)^2\right]}}.$$

Let us define $\mathbb{R}_{\geq 0} \ni \Omega = \omega^2$. In order to find the critical points Ω^*, we apply the natural logarithm to the argument of the square root and differentiate with respect to Ω:

$$\frac{\mathrm{d}}{\mathrm{d}\Omega}\left\{\ln\left(\Omega + \left(k_{3f}^{1}\right)^2\right) - \ln\left(\Omega + \left(\mu^{1}\right)^2\right) - \ln\left(\Omega + \left(k_2^{1}\right)^2\right)\right\}\Big|_{\Omega=\Omega^*} = 0.$$

Solving the foregoing equation for Ω^*, yields

$$\Omega^* = -\left(k_{3f}^1\right)^2 \pm \sqrt{\left[\left(k_{3f}^1\right)^2 - \left(k_2^1\right)^2\right]\left[\left(k_{3f}^1\right)^2 - \left(\mu^1\right)^2\right]}. \tag{26}$$

For simplicity, let us consider the case in which

$$k_{3f}^1 > k_2^1. \tag{27}$$

When $k_{3f}^1 > \mu^1$, the radicand in (26) is positive, but smaller than $\left(k_{3f}^1\right)^4$ resulting in a negative Ω^*. On the other hand, if $k_{3f}^1 < \mu^1$, the radicand is negative and Ω^* becomes complex. That is to say, when $k_{3f}^1 > k_2^1$, there is no positive real solution for Ω^*. Therefore, the global supremum in equation (25) is obtained at either $\Omega = 0$ or $\Omega = \infty$. By substitution, we note that this supermum is achieved at $\Omega = 0$. From (25) we have

$$\gamma^1 = \left|\frac{\sigma^1 k_{3f}^1}{\mu^1 k_2^1}\right|. \tag{28}$$

In the following, we consider the definition of the parameters to derive local stability conditions of each steady state in (18).

1. **Off Steady State**
   Considering the definition of the *off steady state* in (18a) and the definitions in (21) for σ^1 and μ^1, the $\mathcal{L}_2$ gain of the system in (28) reduces to

   $$\gamma_{\text{off}}^1 = \frac{k_1^1 k_{3b}^1}{k_2^1 k_{3f}^1}.$$

   The Small Gain Theorem (2) guarantees stability when $\gamma_{\text{off}}^1 < 1$, hence the *off steady state* is locally stable if

   $$k_2^1 k_{3f}^1 - k_1^1 k_{3b}^1 > 0. \tag{29}$$

2. **On Steady State**
   Likewise, taking into account the definitions in (21) evaluated at this steady state (18b), the $\mathcal{L}_2$ gain of the system in (28) becomes

   $$\gamma_{\text{on}}^1 = \frac{k_2^1 k_{3f}^1}{k_1^1 k_{3b}^1},$$

   leading to the following sufficient condition for stability for the *on steady state*:

   $$k_1^1 k_{3b}^1 - k_2^1 k_{3f}^1 > 0. \tag{30}$$

Note that the stability conditions for the *off* and *on steady states* in (29) and (30), respectively, are mutually exclusive. That is to say, only one steady state is stable for any chosen parameter values that complies with (27). We furthermore note that the stability condition in (30) coincides with the condition for the steady state concentration of the active proteins in (18b) to be positive, and therefore biologically meaningful.

In the next sections, we will also demonstrate that these stability conditions are not only sufficient, but also necessary. There, we will also generalise these results to a protein activation mechanism with p activation steps as depicted in Figure 1B.

5 Equilibria of Positive Feedback Loops of Arbitrary Length

5.1 Sequential Protein Activation Mechanism Definition

We now calculate the steady states for a sequential protein activation of arbitrary length. We consider that the $i+1th$ active protein $\left(A^{i+1}\right)$ activates the ith inactive protein $\left(P^i\right)$, by the following reaction network

$$P^i + A^{i+1} \xrightarrow{k_1^i} A^i + A^{i+1}, \tag{31a}$$

$$A^i \xrightarrow{k_2^i} 0, \tag{31b}$$

$$P^i \underset{k_{3b}^i}{\overset{k_{3f}^i}{\rightleftharpoons}} 0. \tag{31c}$$

The latter two reactions in (31) again describe degradation of the ith active form of the protein and protein turnover of the inactive form, respectively. To close the activation loop, the first active protein (A^1) is assumed to activate the last inactive protein (P^p), according to the mechanism shown in Figure 1B. In other words, the index i should be understood within arithmetic modulo p.

By letting

$$\mathbf{c} = \left(\mathbf{c}^{1T} \ \dots \ \mathbf{c}^{pT}\right)^T \tag{32a}$$

$$\mathbf{c}^i = \left([P^i] \ [A^i]\right)^T, \tag{32b}$$

the stoichiometric matrix and reaction rate vector are given by

$$\mathbf{N} = \operatorname{diag}\left\{\mathbf{N}^1, \mathbf{N}^2, \dots, \mathbf{N}^p\right\}, \tag{33a}$$

$$\mathbf{v}(\mathbf{c}) = \left(\mathbf{v}^1(\mathbf{c}^1, \mathbf{c}^2)^T \quad \mathbf{v}^2(\mathbf{c}^2, \mathbf{c}^3)^T \quad \dots \quad \mathbf{v}^p(\mathbf{c}^p, \mathbf{c}^1)^T\right)^T \tag{33b}$$

where

$$\mathbf{v}^i(\mathbf{c}^i, \mathbf{c}^{i+1}) = \left(k_1^i c_1^i c_2^{i+1} \quad k_2^i c_2^i \quad k_{3f}^i c_1^i - k_{3b}^i\right)^T. \tag{34}$$

We recall that $\bar{c}_1^i$ and $\bar{c}_2^i$ denote the concentration of the ith inactive and activated protein, respectively. With these definitions, we derive closed-form

formulas for the steady states concentrations of the $2p$ proteins concentrations in terms of the kinetic parameters.

5.2 Calculation of Equilibrium Points

Following the ideas introduced in Section 4.1, we calculate the equilibrium points of the reaction network in (31). We present these results in the theorem below.

Theorem 3 *Consider the reaction network in* (31)*, with the mass-action based reaction rates defined in* (34)*. This reaction network*

i) has two equilibrium points,
ii) specified by the following relation, for all i in $[1, p]$,

$$\textbf{Off steady state }:\bar{\mathbf{c}}^i_{\text{off}} = \begin{pmatrix} \dfrac{k^i_{3b}}{k^i_{3f}} & 0 \end{pmatrix}^T, \tag{35a}$$

$$\textbf{On steady state }:\bar{\mathbf{c}}^i_{\text{on}} = \begin{pmatrix} \dfrac{\vartheta^i + k^i_{3b}}{k^i_{3f}} & -\dfrac{\vartheta^i}{k^i_2} \end{pmatrix}^T, \tag{35b}$$

where

$$\vartheta^{i+1} = \frac{\displaystyle\prod_{j=1}^{p}\psi^j - \prod_{j=1}^{p}\zeta^j}{\displaystyle\prod_{j=1}^{i}\zeta^j \sum_{\ell=i+1}^{p}\left(k^\ell_1 \prod_{j=i+1}^{\ell-1}\psi^j \prod_{j=\ell+1}^{p}\zeta^j\right) + \prod_{j=i+1}^{p}\psi^j \sum_{\ell=1}^{i}\left(k^\ell_1 \prod_{j=1}^{\ell-1}\psi^j \prod_{j=\ell+1}^{i}\zeta^j\right)}, \tag{36}$$

and

$$\psi^j := k^{j+1}_2 k^j_{3f}, \tag{37a}$$

$$\zeta^j := k^j_1 k^j_{3b}. \tag{37b}$$

We note that only the superindex i in k^i_1, k^i_2, k^i_{3f}, and k^i_{3f} is treated as a modulo p integer. Whereas the limits of the sums and products indexes in (36) are integers. Additionally, when the index of the lower bound of the sum (product, respectively) is greater than the upper bound, the sum (product) is defined to be zero (one).

Proof Since the reaction topology is the same for every activation step, we note that $\mathbf{N}^1 = \mathbf{N}^2 = \ldots = \mathbf{N}^p$. The matrix $\mathbf{N}^1$ has already been defined in (10a). A basis for Null($\mathbf{N}$) is given by

$$\mathbf{K} = \operatorname{diag}\left\{\mathbf{K}^1, \mathbf{K}^2, \ldots, \mathbf{K}^p\right\}.$$

Furthermore, we note that $\mathbf{K}^1 = \mathbf{K}^2 = \ldots = \mathbf{K}^p$ with $\mathbf{K}^1$ defined in (13). Now, the equilibrium set will be found by noting that

$$\mathbf{N}\mathbf{v}(\bar{\mathbf{c}}) = \mathbf{0} \quad \Leftrightarrow \quad \mathbf{N}^i\mathbf{v}^i\left(\bar{\mathbf{c}}^i, \bar{\mathbf{c}}^{i+1}\right) = \mathbf{0} \quad \forall\, i \in [1, p],$$

which in terms of the null space of $\mathbf{N}^i$, becomes

$$\mathbf{K}^i\boldsymbol{\vartheta}^i = \mathbf{v}^i\left(\bar{\mathbf{c}}^i, \bar{\mathbf{c}}^{i+1}\right).$$

Or *in extenso*, using the definitions of $\mathbf{K}^1$ and $\mathbf{v}^i\left(\bar{\mathbf{c}}^i, \bar{\mathbf{c}}^{i+1}\right)$ in (14) and (34), we get

$$k_1^i\bar{c}_1^i\bar{c}_2^{i+1} = -\vartheta^i \tag{38a}$$

$$k_2^i\bar{c}_2^i = -\vartheta^i \tag{38b}$$

$$k_{3f}^i\bar{c}_1^i - k_{3b}^i = \quad \vartheta^i, \tag{38c}$$

Analogously to the one-tier feedback analysed in Section 4.1, we conclude that the solution for the equation above can be parametrised by ϑ^i as

$$\bar{c}_1^i = \frac{\vartheta^i + k_{3b}^i}{k_{3f}^i}, \tag{39a}$$

$$\bar{c}_2^i = -\frac{\vartheta^i}{k_2^i}. \tag{39b}$$

Substituting the above formulas into (38a), leads to

$$\vartheta^{i+1} = \frac{\alpha^i\vartheta^i}{1 + \beta^i\vartheta^i} = \frac{\alpha^i\mathrm{n}\left(\vartheta^i\right)}{\mathrm{d}\left(\vartheta^i\right) + \beta^i\mathrm{n}\left(\vartheta^i\right)}. \tag{40}$$

Here, $\mathrm{n}\left(\vartheta^i\right)$ and $\mathrm{d}\left(\vartheta^i\right)$ denote the numerator and denominator of the rational term ϑ^i. Moreover, we have defined

$$\alpha^i := \frac{k_2^{i+1}k_{3f}^i}{k_1^ik_{3b}^i} = \frac{\psi^i}{\zeta^i}, \tag{41a}$$

$$\beta^i := \frac{1}{k_{3b}^i}. \tag{41b}$$

The constants ψ^i and ζ^i are defined in (37). To find a closed-form expression for all $\mathbf{c}^i$, we note that from (40) ϑ^2, ϑ^3 and ϑ^4 can be expressed in terms of ϑ^1, as follows

$$\vartheta^2 = \alpha^1\frac{\vartheta^1}{1 + \beta^1\vartheta^1},$$

$$\vartheta^3 = \alpha^1\alpha^2\frac{\vartheta^1}{1 + \left[\beta^1 + \alpha^1\beta^2\right]\vartheta^1},$$

$$\vartheta^4 = \frac{\vartheta^1\prod_{j=1}^3\alpha^j}{1 + \left[\beta^1 + \alpha^1\beta^2 + \alpha^1\alpha^2\beta^3\right]\vartheta^1}.$$

In general

$$\vartheta^{i+1} = \frac{\vartheta^1 \prod_{j=1}^{i} \alpha^j}{1 + \left[\sum_{\ell=1}^{i} \beta^\ell \prod_{j=1}^{\ell-1} \alpha^j\right] \vartheta^1}. \tag{42}$$

When $i = p$ the expression above becomes

$$\vartheta^1 = \frac{\vartheta^1 \prod_{j=1}^{p} \alpha^j}{1 + \left[\sum_{\ell=1}^{p} \beta^\ell \prod_{j=1}^{\ell-1} \alpha^j\right] \vartheta^1}. \tag{43}$$

Solving (43) for ϑ^1, we obtain

$$\begin{aligned} 0 &= \vartheta^1 \left(\vartheta^1 - \frac{\prod_{j=1}^{p} \alpha^j - 1}{\sum_{\ell=1}^{p} \beta^\ell \prod_{j=1}^{\ell-1} \alpha^j} \right) \\ 0 &= \vartheta^1 \left(\vartheta^1 - \frac{\prod_{j=1}^{p} \psi^j - \prod_{j=1}^{p} \zeta^j}{\sum_{\ell=1}^{p} k_1^\ell \prod_{j=1}^{\ell-1} \psi^j \prod_{j=\ell+1}^{p} \zeta^j} \right). \end{aligned} \tag{44}$$

The constants ζ^j and ψ^j above were defined in (37). Equation (44) is a second order polynomial in ϑ^1. Substituting the trivial solution $\vartheta^1 = 0$ of (44) into (42) leads to $\vartheta^i = 0$ for all i, defining the *off steady state*.

In order to find the solution for the ϑ^is defining the *on steady state*, we note that we can rewrite (42) as

$$\vartheta^{i+1} = \frac{\mathrm{n}\left(\vartheta^1\right) \prod_{j=1}^{i} \alpha^j}{\mathrm{d}\left(\vartheta^1\right) + \left[\sum_{\ell=1}^{i} \beta^\ell \prod_{j=1}^{\ell-1} \alpha^j\right] \mathrm{n}\left(\vartheta^1\right)}.$$

Substituting the non-trivial root of (44) into the equation above and considering (41a) and (41b) yield

$$\vartheta^{i+1} = \frac{\prod_{j=1}^{p} \psi^j - \prod_{j=1}^{p} \zeta^j}{\prod_{j=1}^{i} \zeta^j \sum_{\ell=i+1}^{p} \left(k_1^\ell \prod_{j=i+1}^{\ell-1} \psi^j \prod_{j=\ell+1}^{p} \zeta^j \right) + \prod_{j=i+1}^{p} \psi^j \sum_{\ell=1}^{i} \left(k_1^\ell \prod_{j=1}^{\ell-1} \psi^j \prod_{j=\ell+1}^{i} \zeta^j \right)}.$$

□

We conclude this section with a remark on the nonnegativity of the steady states. For the *off steady state*, according to equation (39) and given the positivity of the kinetic parameters k_j^i, the concentrations of all inactive proteins are positive and those of all active proteins are zero. Consequently, the *off steady state* is biologically meaningful for all possible kinetic parameter values.

To investigate the positivity of the concentrations of the *on steady state*, we note that, from (38a) and (38b), $\bar{c}_1^i$ may be expressed as the ratio of positive terms (see the definition of $\mathrm{d}\left(\vartheta^{i+1}\right)$ in (36)):

$$\begin{aligned}\bar{c}_1^i &= \frac{k_2^{i+1}}{k_1^i}\frac{\vartheta^i}{\vartheta^{i+1}},\\ \bar{c}_1^i &= \frac{k_2^{i+1}}{k_1^i}\frac{\mathrm{d}\left(\vartheta^{i+1}\right)}{\mathrm{d}\left(\vartheta^i\right)}.\end{aligned} \tag{45}$$

Hence, we can be assured that all concentrations of the inactive proteins for the *on steady state* are positive. In turn, for all the concentrations of the active proteins to be positive, we require the numerator ϑ^{i+1} in (36) to be negative since the denominator of ϑ^{i+1} in (36) is positive. As for every i, the numerator of ϑ^{i+1} is the same, all the active proteins are positive when

$$\prod_{j=1}^{p} k_1^j k_{3b}^j - \prod_{j=1}^{p} k_2^j k_{3f}^j > 0. \tag{46}$$

Here we used the relation (41) and replaced $j+1$ by j in the second product by exploiting the modularity of the product with respect to p. Furthermore, this condition is independent of i, therefore unspecific for the actual protein and, consequently, a general condition for a meaningful *on steady state*.

We conclude by stating that the existence of a biologically meaningful *on steady state* requires that the *product of all the synthesis and activation rates of the inactive proteins is greater than the product of all degradation rates of the active and inactive proteins.*

In the next section, we characterise the stability of the steady states in (35), by means of procedure used in Section 4.2.

6 Local Stability Analysis of Positive Feedback Loops of Arbitrary Length

As exemplified in Section 4.2, we now present local stability conditions for both steady states of the reaction system in (31) and express these conditions in terms of the kinetic parameters. The linearisation of the entire system (33) will therefore be expressed as an interconnection of p linear subsystems. For each subsystem, the $\mathcal{L}_2$ gain will be calculated using Theorem 1. Further application of the Small Gain Theorem (Theorem 2) leads to sufficient conditions for the stability of the *off* and *on steady states*. A comparable approach using the Small Gain Theorem has recently been provided for local instability analysis to investigate periodic oscillations in gene regulatory networks [15].

6.1 Linearisation of the p-tier Feedback Loop Model

The linearisation of the nonlinear model in (2) has the form

$$\frac{\mathrm{d}}{\mathrm{d}t}\mathbf{e} = \mathbf{A}\mathbf{e}, \tag{47}$$

where $\mathbf{e} = \mathbf{c} - \bar{\mathbf{c}}$ are the deviation coordinates relative to the steady state $\bar{\mathbf{c}}$, and $\mathbf{A}$ is the Jacobian of the system (2). With the definitions of the stoichiometric matrix and reaction rate given in (33), this Jacobian is given by

$$\mathbf{A} := \frac{\mathrm{d}}{\mathrm{d}\mathbf{c}}\mathbf{N}\mathbf{v}(\mathbf{c}) = \begin{pmatrix} \mathbf{A}^{11} & \mathbf{A}^{12} & \mathbf{0} & \dots & \mathbf{0} \\ \mathbf{0} & \mathbf{A}^{22} & \mathbf{A}^{23} & \dots & \mathbf{0} \\ \ddots & \ddots & \ddots & \ddots & \ddots \\ \mathbf{A}^{p1} & \mathbf{0} & \mathbf{0} & \dots & \mathbf{A}^{pp} \end{pmatrix}, \tag{48}$$

with the block matrices defined as

$$\mathbf{A}^{ii} := \frac{\mathrm{d}}{\mathrm{d}\mathbf{c}^i}\mathbf{N}^i\mathbf{v}^i\left(\mathbf{c}^i, \mathbf{c}^{i+1}\right) = \begin{pmatrix} -\mu^i & 0 \\ \mu^i - k_{3f}^i & -k_2^i \end{pmatrix} \tag{49a}$$

$$\mathbf{A}^{i,i+1} := \frac{\mathrm{d}}{\mathrm{d}\mathbf{c}^{i+1}}\mathbf{N}^i\mathbf{v}^i\left(\mathbf{c}^i, \mathbf{c}^{i+1}\right) = \sigma^i \begin{pmatrix} 0 & -1 \\ 0 & 1 \end{pmatrix}, \tag{49b}$$

where

$$\sigma^i := k_1^i \bar{c}_1^i \tag{50a}$$

$$\mu^i := k_1^i \bar{c}_2^{i+1} + k_{3f}^i. \tag{50b}$$

Note that $\mathbf{A}^{i,i+1}$ can be expressed as the product $\mathbf{A}^{i,i+1} = \mathbf{B}^i\mathbf{C}$, where

$$\mathbf{B}^i := \sigma^i \begin{pmatrix} -1 \\ 1 \end{pmatrix}, \tag{51a}$$

$$\mathbf{C} := \begin{pmatrix} 0 & 1 \end{pmatrix}. \tag{51b}$$

Therefore, the linearisation in (47) can be expressed as the interconnection of p systems of the form (cf. Eq. (4))

$$\frac{\mathrm{d}}{\mathrm{d}t}\mathbf{e}^i = \mathbf{A}^{ii}\mathbf{e}^i + \mathbf{B}^i u^i, \tag{52a}$$

$$y^i = \mathbf{C}\mathbf{e}^i. \tag{52b}$$

Here $\mathbf{e}^i = \mathbf{c}^i - \bar{\mathbf{c}}^i$ is the species concentration referred to the steady state $\bar{\mathbf{c}}_i$. From the interconnection topology in (31) and the order of states as defined in (32), we note that

$$u^i = y^{i+1}. \tag{53}$$

In addition, the transfer function of the system in (52), as defined in (6), is given by

$$h^i(s) = \sigma^i \frac{s + k_{3f}^i}{(s + \mu^i)(s + k_2^i)}. \tag{54}$$

By splitting the linearisation of the reaction network in (47) into p subsystems of the form (52), we can analyse the input-output behaviour of p systems separately and, then, infer conditions on the stability of each steady state of the entire interconnected system (47). These ideas, motivated in Section 4.2 for $p = 1$, will lead to local stability conditions of (47) and are summarised in Theorem 4. The strategy of the proof is to obtain the $\mathcal{L}_2$ gain of the transfer function of the system (52). Once the gain for the p isolated systems is obtained, we avail of the Small Gain Theorem (Theorem 2) to obtain conditions on the parameters that ensure local stability of the interconnected systems. For application of the Small Gain Theorem, it is sufficient that the individual subsystems are stable. The following lemma states that for all i and both steady states, the transfer function of the *ith* system in (54) is stable.

Lemma 1 *The transfer function $h^i(s)$ in (54) is stable for all $i \in [1, p]$ and for the* off *and* on steady state.

The proof of this Lemma can be found in Appendix 9.1.

6.2 Necessary and Sufficient Criteria for Local Stability of Both States

In the following theorem, we present necessary and sufficient conditions for stability of the interconnection depicted in Figure 1B of p subsystems of the form (52) above which hold for certain conditions of the kinetic parameters.

Theorem 4 *Consider the system in (47) and suppose $\forall\, i \in [1, p]$ that one of the following conditions holds*

$$\text{case 1: } k_{3f}^i \geq k_2^i \quad \text{or} \tag{55a}$$

$$\text{case 2: } k_2^i > k_{3f}^i, \quad \mu^i \geq k_{3f}^i, \quad \text{and} \quad \frac{1}{\left(k_{3f}^i\right)^2} < \frac{1}{\left(k_2^i\right)^2} + \frac{1}{(\mu^i)^2}, \tag{55b}$$

with μ^i as defined in (50). Then, the system in (47) is ***stable if and only if***

$$\prod_{i=1}^{p} \frac{\sigma^i k_{3f}^i}{\mu^i k_2^i} < 1. \tag{56}$$

Proof In Lemma 1 we have shown that every subsystem (54) is stable, hence the cascade connection of the p subsystems leads to a stable system. Thus we can use the Small Gain Theorem (2) to determine the condition under which the closed-loop depicted in Figure 2, where $\mathbf{H}(s) = \prod_{i=1}^{p} h^i(s)$, is stable. That

is to say, for the circular connection of the p subsystems to be stable, we require

$$\left|\left|\prod_{i=1}^{p} h^i(s)\right|\right| \leq \prod_{i=1}^{p} ||h^i(s)|| < 1. \tag{57}$$

Now, we compute the $\mathcal{L}_2$ gain of the individual subsystems. From Theorem 1 the $\mathcal{L}_2$ gain of $h^i(s)$ is given by

$$\gamma^i = \left|\sigma^i\right| \sup_{\omega\in\mathbb{R}} \sqrt{\frac{\omega^2 + \left(k_{3f}^i\right)^2}{\left[\omega^2 + \left(\mu^i\right)^2\right]\left[\omega^2 + \left(k_2^i\right)^2\right]}}. \tag{58}$$

Analogously to the case in Section 4.2 where autoactivation ($p = 1$) was studied, the gain γ^i is maximum under the condition

$$\Omega^* = -\left(k_{3f}^i\right)^2 \pm \sqrt{\left[\left(k_{3f}^i\right)^2 - \left(k_2^i\right)^2\right]\left[\left(k_{3f}^i\right)^2 - \left(\mu^i\right)^2\right]}. \tag{59}$$

for $\Omega = \omega^2 \in \mathbb{R}_{\geq 0}$.

To find the supremum of (58), we again investigate the existence of positive real solutions of (59). Once more, we will conclude that no local maximum exists and the global extremum has to be found at the boundaries. We first focus on *case 1* where condition (55a) is met. In this case, two subcases have to be considered. First, when $k_{3f}^i \geq \mu^i$ holds, the radicand will be less than $(k_{3f}^i)^4$, resulting in a negative Ω^*. In contrast when the condition $k_{3f}^i \leq \mu^i$ is met, the radicand in (59) is negative resulting in a complex Ω^*.

For *case 2*, where condition (55a) is not met, the radicand is non-negative when both relations $k_2^i > k_{3f}^i$ and $\mu^i \geq k_{3f}^i$ hold, leading to a real value for the square root. Nevertheless under these conditions Ω^* is negative when

$$\left(k_{3f}^i\right)^2 > \sqrt{\left[\left(k_{3f}^i\right)^2 - \left(k_2^i\right)^2\right]\left[\left(k_{3f}^i\right)^2 - \left(\mu^i\right)^2\right]}.$$

The foregoing condition is equivalent to

$$\frac{1}{\left(k_{3f}^i\right)^2} < \frac{1}{\left(k_2^i\right)^2} + \frac{1}{\left(\mu^i\right)^2}.$$

In conclusion, no positive real solution of (59) exists under either condition (55a) or (55b). Therefore, the supremum in equation (58) is obtained for either $\Omega = 0$ or $\Omega = \infty$. Indeed, the maximum value is achieved for $\Omega = 0$. Hence, from (58) we obtain

$$\gamma^i = \left|\frac{\sigma^i k_{3f}^i}{\mu^i k_2^i}\right|. \tag{60}$$

The Small Gain Theorem 2 implies that the closed loop system is stable if

$$\gamma := \prod_{i=1}^{p} \left| \frac{\sigma^i k_{3f}^i}{\mu^i k_2^i} \right| < 1. \tag{61}$$

where we have considered the definition of γ^i in (60).

To prove the necessary condition of Theorem 4, we firstly note that the closed loop transfer function of the interconnected system is given by

$$h(s) := \frac{h^p}{1 - \prod_{i=1}^{p} h^i(s)}. \tag{62}$$

Let $\gamma \geq 1$. From (62), the characteristic equation is given by

$$\begin{aligned} q(s) &:= 1 - \prod_{i=1}^{p} h^i(s), \\ &= 1 - \prod_{i=1}^{p} \sigma^i \frac{s + k_{3f}^i}{(s + \mu^i)(s + k_2^i)}, \end{aligned}$$

where we have used the definition of the transfer function in (54). The limit of the equation above as s approaches to $+\infty$ and 0 yields

$$\begin{aligned} q(\infty) &= 1 \\ q(0) &= 1 - \gamma. \end{aligned}$$

Hence there must be at least one root of the characteristic equation with a non-negative real part, when $\gamma \geq 1$. □

The theorem above provides necessary and sufficient conditions for the local stability of each steady state. We now consider the definition of these steady states and express, for each steady state, the stability condition in (56) in terms of the kinetic parameters of the reaction network in (31). The results are summarised in the following corollary whose proof can be found in Appendix 9.2.

In the following, we denote $\mathbf{A}_{\text{off}}$ as the Jacobian in (48) evaluated at the *off steady state*, defined in (35a). The definition of $\mathbf{A}_{\text{on}}$ follows similarly.

Corollary 1 *Consider the system* (47)*:*

1. *The* **off steady state** *of* (47) *is* ***stable if and only if***

$$\det\left(\mathbf{A}_{\text{off}}\right) = \prod_{i=1}^{p} k_2^i k_{3f}^i - \prod_{i=1}^{p} k_1^i k_{3b}^i \; > 0. \tag{63a}$$

2. Provided $\forall\, i \in [1,p]$ *one of the following conditions holds*

$$\begin{aligned} &\text{case 1:} \quad k_{3f}^i \geq k_2^i \qquad\qquad\qquad \text{or} \\ &\text{case 2:} \quad k_2^i > k_{3f}^i \quad \text{and} \quad \tfrac{1}{\left(k_{3f}^i\right)^2} < \tfrac{1}{\left(k_2^i\right)^2} + \tfrac{1}{(\mu^i)^2}, \end{aligned} \tag{63b}$$

then the **on steady state** *is stable* ***if and only if***

$$\det\left(\mathbf{A}_{\text{on}}\right) = \prod_{i=1}^{p} k_1^i k_{3b}^i - \prod_{i=1}^{p} k_2^i k_{3f}^i \ > 0. \tag{63c}$$

From the corollary above we find that the stability conditions for the *off steady state* and *on steady state* are mutually exclusive. Since for all parameter sets satisfying (63b) these conditions are both sufficient and necessary for stability of the respective steady state, exactly one steady state will be stable in this parameter regime. Comparing (63c) and (46), we note that stability of the *on steady state* is equivalent to this state having positive concentrations, therefore being biologically meaningful.

6.3 Sufficient conditions for local stability of the *on steady state* for the remaining sets of parameters

Although Corollary 1 provides full characterisation of the stability of the closed-loop system, its validity for the *on steady state* depends on the kinetic parameters conditions in (55). For completeness, in Theorem 5 we analyse the stability of the *on steady state*, for the kinetic parameters not considered in (55). More specifically, we assume that for some i the condition (55) is violated. Nevertheless, also for these nodes an upper bound for γ can be derived by assessing positive real solution for Ω^* in (59). Results are formulated in the Theorem below with its proof given in Appendix 9.4.

Theorem 5 *Let for some* $i \in [1,p]$

$$k_2^i > k_{3f}^i, \tag{64a}$$

$$\mu_{\text{on}}^i > k_{3f}^i, \tag{64b}$$

$$\frac{1}{\left(k_{3f}^i\right)^2} > \frac{1}{\left(k_2^i\right)^2} + \frac{1}{\left(\mu_{\text{on}}^i\right)^2}. \tag{64c}$$

Then the on steady state *of the system in* (47) *is* ***stable if***

$$\prod_{i=1}^{p} \frac{k_2^{i+1} k_{3f}^i}{k_1^i k_{3b}^i} < \prod_{i=1}^{p} \theta^i, \tag{65}$$

where

$$\theta^i = \begin{cases} \frac{k_{3f}^i}{\mu_{\text{on}}^i}\sqrt{1-\left(\frac{k_{3f}^i}{k_2^i}\right)^2} + \frac{k_{3f}^i}{k_2^i}\sqrt{1-\left(\frac{k_{3f}^i}{\mu_{\text{on}}^i}\right)^2} & ,\forall\, i \text{ which satisfy (64)} \\ 1 & ,\text{otherwise.} \end{cases} \tag{66}$$

A more conservative, yet tractable, stability criterion is given by

$$\prod_{i=1}^{p} \frac{k_2^{i+1} k_{3f}^i}{k_1^i k_{3b}^i} < \prod_{i=1}^{p} \nu^i, \tag{67}$$

where,

$$\nu^i = \begin{cases} \left(\dfrac{k_{3f}^i}{k_2^i}\right)^2 & , \forall\, i \text{ which satisfy (64)} \\ 1 & , \text{otherwise.} \end{cases} \tag{68}$$

Moreover, the on steady state *will be unstable if* (63c) *does not hold.*

Both conditions (65) and (67), provide a criterion for determining the stability of the *on steady state*, when some of the subsystems in the loop satisfy (64). However, some parameters may not satisfy (65) and (67), while their stability also cannot be excluded by Corollary 1 (Condition (63c)). For these parameters, no statement about stability of the *on steady state* of system (47) can be given using our approach.

We further note that even when only some i fulfil the condition $k_2^i > k_{3f}^i$, the stability criterion in (67) can be applied for all i. Consequently, Theorem 5 is often the preferred option to Theorem 4 when analysing stability for the *on steady state*. While this choice may lead to a more conservative estimation of stability and does not allow to prove necessity of stability criteria, the parameter space covered is more extensive and a tedious case-by-case analysis of the parameter conditions necessary for applying the appropriate theorem and subcases can be avoided.

In conclusion, in this section we performed *local* stability analysis of (47) and stated our results for certain conditions of the parameter space. The results described in Theorem 4 provides necessary and sufficient conditions for stability of the *off* and *on steady state*. In turn, Theorem 5 presents sufficient stability conditions for the *on steady state*, for cases not accounted for in Theorem 4. In addition, we remark that since we only performed a *local* stability analysis, we have not rigorously ruled out the existence of strange attractors or chaotic behaviours [32]. However, such phenomena were not observed in numerical analysis performed in the context of this work (data not shown). To finalise our study, we avail of the analytical formula for the steady states (35) and also apply the stability criterion in (67) *for all* i to investigate the caspase-3 activation in the caspase-3/6/8 feedback loop.

7 Application to Caspase Activation in Programmed Cell Death

The analyses in the previous sections demonstrated that the existence and the stability of the *on steady state*, as well as the concentrations of its active proteins are characterised by the product of the kinetic constants k_j^i. Like any other product, this condition crucially depends on each of its factors which

denote biochemical activity of the feedback k_1^i, the activity of protein degradation k_2^i or protein expression (the fraction k_{3f}^i/k_{3b}^i) for each protein in the loop [16].

We envisioned that small variations in such constants strongly affect the existence and the stability properties of the *on steady state* and the concentration of active proteins. In particular, we assumed that any bottleneck in this loop (such as a weak feedback link or a protein expressed at low levels) would significantly determine whether or not the loop would lead to an activation of the entire protein chain and how extensive the protein activation would be. To this end, we focused on the process of caspase-dependent programmed cell death (apoptosis) and illustrated how a three-tier feedback loop can act as a signal amplifier. During execution of apoptosis, a three-tier positive feedback has been shown to occur downstream of caspase-3 activation. In this loop, caspase-3 cleaves and activate caspase-6, while caspase-6 activates caspase-8 and caspase-8 closes the feedback by cleaving caspase-3 [7,18] (Figure 3A). Moreover, caspase-6 has been shown to be expressed at lower levels compared to both other caspases [35,4], suggesting it to be the major bottleneck in the loop.

We therefore investigated how fine tuning of the caspase-6 synthesis rate (k_{3b}^2), and therefore a small change in caspase-6 expression levels, influenced the steady state expression levels of the major effector in this loop, the active caspase-3. We modelled this caspase-3/6/8 feedback as described previously [35] taking all kinetic constants from their supplementary data. We then varied the caspase-6 synthesis rate and studied the expression of active caspase-3 at steady state (Figure 3A; dashed arrow for variation of caspase-6; solid arrow for output of caspase-3). To calculate these equilibria we exploited our analytical formula (35) leading to the following expression for steady state levels of active caspase-3

$$\bar{C}_{3a} = \frac{1.8 \times 10^{25} k_{3b}^2 - 1.5 \times 10^{15}}{2.2 \times 10^{26} k_{3b}^2 + 4.8}, \tag{69}$$

which is depicted in Figure 3B. We note that local stability condition for the *off steady state* is given by (see Theorem 4)

$$k_{3b}^2 < 8.36 \times 10^{-11} [\mu M/min].$$

When this threshold is exceeded, the *on steady state* is positive. In order to determine the stability of the *on steady state*, we note that $k_2^i > k_{3f}^i$, as can be seen in the supplemental material of [35]. Hence, we may use the criterion in (67) for all i, to determine the stability of the *on steady state*. As a function of k_{3b}^2, (67) becomes

$$k_{3b}^2 > \frac{1}{k_{3b}^1 k_{3b}^3} \prod_{i=1}^{3} \frac{\left(k_2^i\right)^3}{k_1^i k_{3f}^i} = 9.05 \times 10^{-10} [\mu M/min]. \tag{70}$$

As confirmed by the simulations in the panel Figure 3D, the variation of k_{3b}^2 in agreement with the threshold in (70), yields stable *on steady states*.

To determine the range in which a variation of k_{3b}^2 yields a large effect on the location of the steady state concentration of active caspase-3, we analyse the sensitivity of $\bar{C}_{3a}$ with respect to k_{3b}^2 by

$$\frac{\partial \bar{C}_{3a}}{\partial k_{3b}^2}\frac{k_{3b}^2}{\bar{C}_{3a}} = \frac{5.8\times 10^{48}k_{3b}^2}{(2.2\times 10^{26}k_{3b}^2+4.8\times 10^{17})\,(1.1\times 10^{31}k_{3b}^2+9.6\times 10^{20})}. \quad (71)$$

We present the bi-logarithmic plot of the expression above in Figure 3C, where we note that for a variation of k_{3b}^2 between 5×10^{-9} and $8.36\times10^{-11}[\mu M/min]$, the amount of active caspase $\bar{C}_{3a}$ was markedly amplified ($\frac{\partial \bar{C}_{3a}}{\partial k_{3b}^2}\frac{k_{3b}^2}{\bar{C}_{3a}} > 1$). In contrast, variations of k_{3b}^2 at regions larger than 5×10^{-9}, had a modest effect on the amount of $\bar{C}_{3a}$ when k_{3b}^2 increases. Motivated by this observation, in Figure 3D we present the steady state concentration of active caspase-3 (C_{3a}) and its concentrations in time $C_{3a}(t)$, under a sudden variation of the production rate of k_{3b}^2. In the first case D.1, a relatively small variation of the caspase-6 production rate k_{3b}^2 led to a pronounced change in the amount of active caspase-3 (at steady state) C_{3a} (Figure 3D.1). When the caspase-6 production rate (k_{3b}^2) was varied within a different, and by absolute means even larger, concentration range (see right vertical axis of Figure 3D.2), only a small effect in the expression levels of caspase-3 was observed. Taken together, these results suggest that within certain parameter ranges, an intermediary node in a feedback such as caspase-6 may act as an amplifier, similar to a molecular transistor.

8 Discussion

In this study, we focused on a mathematical treatment of the dynamical equations governing positive feedback loops of arbitrary length under the consideration of protein production and degradation. We derived exact formulas for steady state concentrations and exact stability conditions for these steady states and found that, irrespectively of the chain length, a maximum of two steady states is possible. These states represent either an *off steady state* where all concentration of active proteins are zero or, on the contrary, an *on steady state* where the active versions of all the proteins are present. Under the conditions described in Corollary 1, the *on steady state* was stable as long as it had a positive value, whereas the *off steady state* became unstable. In turn, when the *off state* was determined to be stable, no meaningful *on steady state* was predicted. For completeness, Theorem 5 provided sufficient stability results, for the cases excluded in Theorem 4. As the conditions for stability and existence of both states only depended on kinetic parameters, we conclude that such feedback loops convert any *analogue* changes of kinetic parameters into *digital, on/off* switch in the resulting signalling.

We have obtained mathematical expressions that relate kinetic parameters to activity and stability of the resulting pathway of the entire loop. Kinetic parameters describe enzymatic activity, protein production and degradation

[16]. Variations in protein production and degradation may be imposed by variations of the cell's transcriptional machinery and/or of its proteasomal activity. Enzyme activities vary as a result of changes of pH and temperature [20]. Likewise, pharmacological interventions may target enzyme activity, protein production and degradation. Our analytical results therefore provide an easy means to study dose-responses in pharmacology or robustness of a signalling programme against physiological changes.

We have analytically investigated how feedback loops with larger chain lengths introduce a higher sensitivity in the responding signalling pathway. We found that the activity of the feedback depends on expression levels and activity of all nodes in a multiplicative manner. To illustrate the consequences of this, potentially significant dependency on each node, we studied a three-tier feedback loop of caspase-activation in apoptosis. Results of this example demonstrated that a small modulation of the lowly expressed, intermediary node caspase-6 can markedly influence activity of caspase-3. It is therefore appealing to look at such feedback loops as 'molecular transistors'. Similar to electrical transistors, molecular transistors may amplify weak input signals. Likewise, these molecular transistors may act as a robust switch that shut off activity of the feedback when expression levels of one intermediary node fall below a certain threshold, resulting in an non-existent *on steady state*.

The molecular transistors described above may be convenient in cases of spatial signal transduction within large cells such as skeletal muscle cells or neurones. Here, small gradients of an intermediary protein such as caspase-6 within a cell can either amplify the entire signal or lead to robust switch between activity and inactivity of the loop. This allows the cell to create a location dependent response such as location-dependent caspase activation without investing much effort in keeping up large gradients in protein expression and, therefore, investing in active transport processes. In this context it is interesting to note that localised, but robust caspase-activation has been identified in neurones [34, 22]. Likewise, caspase-6 has also been shown to be involved in neuronal apoptosis, while being dispensable for apoptosis in other cells [26, 13, 29].

In conclusion, even though feedback loops with longer chain lengths may be underrepresented in protein and transcriptional networks of prokaryotes [2] their higher sensitivity as discussed within this paper makes them likely to be beneficial for other cellular contexts. Even in prokaryotes, higher variability is beneficial when changes in external cues need to be integrated and, indeed, larger feedbacks are overrepresented in pathways for chemotaxis and biofilm production [25]. In eukaryotic cells, signalling is more complex and has to respond to a greater variety and to more subtle changes of environmental cues, suggesting the need for higher degree of variability in and richer vocabularity of the signalling response.

9 Appendix

In this section, we present three proofs required in Section 6, to prove the local stability of the *off* and *on steady state*.

9.1 Proof of Lemma 1

Proof From $h^i(s)$ in (54), we note that the roots of its characteristic polynomial are all negative if

$$\mu^i > 0. \tag{72}$$

In the following, we show that μ^i is positive for both steady states and for all i.

1. **Off Steady State**
   Considering the definition of the *off steady state* in (35a) and the definition of σ^i and μ^i, (72) becomes

$$\mu^i_{\text{off}} = k^i_{3f} > 0.$$

2. **On Steady State**
   The *on steady state* is given by (35b), which is parametrised by ϑ^{i+1} defined in (36). We note that (39b) allows us to express μ^i_{on} in (50) as

$$\mu^i_{\text{on}} = k^i_1 \bar{c}_2^{i+1} + k^i_{3f} = \frac{k_2^{i+1} k^i_{3f} \mathrm{d}\left(\vartheta^{i+1}\right) - k^i_1 \mathrm{n}\left(\vartheta^{i+1}\right)}{k_2^{i+1} \mathrm{d}\left(\vartheta^{i+1}\right)}. \tag{73}$$

   Furthermore, we claim

$$k_2^{i+1} k^i_{3f} \mathrm{d}\left(\vartheta^{i+1}\right) = \mathrm{d}\left(\alpha^i\right) \mathrm{d}\left(\vartheta^i\right) + k^i_1 \mathrm{n}\left(\vartheta^{i+1}\right). \tag{74}$$

   We provide a proof of this statement in Claim 1, below. Hence μ^i in (73) becomes

$$\mu^i_{\text{on}} = \frac{\mathrm{d}\left(\alpha^i\right) \mathrm{d}\left(\vartheta^i\right)}{k_2^{i+1} \mathrm{d}\left(\vartheta^{i+1}\right)} > 0 \quad \forall \quad i \in [1, p]. \tag{75}$$

□

Now, we present the proof of (74).

Claim 1 *For all* $i \in [1, p]$

$$k_2^{i+1} k^i_{3f} d\left(\vartheta^{i+1}\right) = d\left(\alpha^i\right) d\left(\vartheta^i\right) + k^i_1 n\left(\vartheta^{i+1}\right),$$

where α^i *has been defined in* (41a).

Proof The strategy of the proof is to rewrite $\mathrm{d}\left(\vartheta^{i+1}\right)$ in terms of $\mathrm{d}\left(\vartheta^{i}\right)$. From (36), we have

$$\begin{aligned}
\mathrm{n}\left(\alpha^{i}\right)\mathrm{d}\left(\vartheta^{i+1}\right) =& \mathrm{n}\left(\alpha^{i}\right)\prod_{j=1}^{i}\mathrm{d}\left(\alpha^{j}\right)\sum_{\ell=i+1}^{p}\left(k_1^{\ell}\prod_{j=i+1}^{\ell-1}\mathrm{n}\left(\alpha^{j}\right)\prod_{j=\ell+1}^{p}\mathrm{d}\left(\alpha^{j}\right)\right)\\
&+\mathrm{n}\left(\alpha^{i}\right)\prod_{j=i+1}^{p}\mathrm{n}\left(\alpha^{j}\right)\sum_{\ell=1}^{i}\left(k_1^{\ell}\prod_{j=1}^{\ell-1}\mathrm{n}\left(\alpha^{j}\right)\prod_{j=\ell+1}^{i}\mathrm{d}\left(\alpha^{j}\right)\right)\\
=&\prod_{j=1}^{i}\mathrm{d}\left(\alpha^{j}\right)\sum_{\ell=i+1}^{p}\left(k_1^{\ell}\prod_{j=i}^{\ell-1}\mathrm{n}\left(\alpha^{j}\right)\prod_{j=\ell+1}^{p}\mathrm{d}\left(\alpha^{j}\right)\right)\\
&+\prod_{j=i}^{p}\mathrm{n}\left(\alpha^{j}\right)\sum_{\ell=1}^{i}\left(k_1^{\ell}\prod_{j=1}^{\ell-1}\mathrm{n}\left(\alpha^{j}\right)\prod_{j=\ell+1}^{i}\mathrm{d}\left(\alpha^{j}\right)\right)\\
=&\mathrm{d}\left(\alpha^{i}\right)\left[\prod_{j=1}^{i-1}\mathrm{d}\left(\alpha^{j}\right)\sum_{k=i}^{p}\left(k_1^{\ell}\prod_{j=i}^{\ell-1}\mathrm{n}\left(\alpha^{j}\right)\prod_{j=\ell+1}^{p}\mathrm{d}\left(\alpha^{j}\right)\right)\right.\\
&\left.+\prod_{j=i}^{p}\mathrm{n}\left(\alpha^{j}\right)\sum_{\ell=1}^{i-1}\left(k_1^{\ell}\prod_{j=1}^{\ell-1}\mathrm{n}\left(\alpha^{j}\right)\prod_{j=\ell+1}^{i-1}\mathrm{d}\left(\alpha^{j}\right)\right)\right]\\
&+k_1^{i}\left[\prod_{j=1}^{p}\mathrm{n}\left(\alpha^{j}\right)-\prod_{j=1}^{p}\mathrm{d}\left(\alpha^{j}\right)\right]\\
=&\mathrm{d}\left(\alpha^{i}\right)\mathrm{d}\left(\vartheta^{i}\right)+k_1^{i}\mathrm{n}\left(\vartheta^{i+1}\right).
\end{aligned}$$

□

9.2 Proof of Corollary 1

Proof The closed-form expressions of $\det\left(\mathbf{A}_{\mathrm{off}}\right)$ and $\det\left(\mathbf{A}_{\mathrm{on}}\right)$ in (63a) and (63c), respectively, are derived in Lemma 4 in Section 9.3.

1. **Off Steady State**
   The *off steady state* is given in (35a).
   We note that when we evaluate the conditions (55b) at the *off steady state* (35a), we obtain

$$k_2^{i} > k_{3f}^{i}, \quad k_{3f}^{i} \geq k_{3f}^{i}, \quad \text{and} \quad \frac{1}{\left(k_{3f}^{i}\right)^{2}} < \frac{1}{\left(k_2^{i}\right)^{2}} + \frac{1}{\left(k_{3f}^{i}\right)^{2}}.$$

   The later two expressions are always satisfied, given the parameters are positive. Now, the former condition $k_2^{i} > k_{3f}^{i}$ combined with the condition $k_2^{i} < k_{3f}^{i}$ in (55a), shows that we can guarantee the local stability of the *off steady state* for all parameter values that satisfy (56). Substituting (35a)

into (56) yields

$$\gamma_{\text{off}} := \prod_{i=1}^{p} \frac{k_1^i k_{3b}^i}{k_2^i k_{3f}^i} < 1, \tag{76}$$

or equivalently

$$\prod_{i=1}^{p} k_2^i k_{3f}^i - \prod_{i=1}^{p} k_1^i k_{3b}^i > 0, \tag{63a}$$

as stated in (63a).

2. **On Steady State**
The *on steady state* is given by (35b), which is parametrised by ϑ^{i+1} defined in (36). Moreover, we recall that

$$\mu_{\text{on}}^i = \frac{\mathrm{d}\left(\alpha^i\right)\mathrm{d}\left(\vartheta^i\right)}{k_2^{i+1}\mathrm{d}\left(\vartheta^{i+1}\right)}. \tag{75}$$

In addition, we note that, with the expressions (38a) and (39b), σ^i in (50) may be rewritten as

$$\sigma_{\text{on}}^i = k_1^i \bar{c}_1^i = \frac{k_2^{i+1}\mathrm{d}\left(\vartheta^{i+1}\right)}{\mathrm{d}\left(\vartheta^i\right)}.$$

With the two former expressions, the stability condition (56) becomes

$$\gamma_{\text{on}} := \prod_{i=1}^{p} \gamma_{\text{on}}^i = \prod_{i=1}^{p} \frac{k_2^{i+1}}{k_2^i} \left(\frac{\mathrm{d}\left(\vartheta^{i+1}\right)}{\mathrm{d}\left(\vartheta^i\right)}\right)^2 \frac{k_2^{i+1} k_{3f}^i}{k_1^i k_{3b}^i} < 1. \tag{77}$$

Consequently, the small gain stability condition in (56) is

$$\prod_{i=1}^{p} k_1^i k_{3b}^i - \prod_{i=1}^{p} k_2^i k_{3f}^i > 0, \tag{63c}$$

where we have taken into account the modularity of the superindex i in k_2^{i+1}.

□

9.3 Closed Form of the Determinant of $\mathbf{A}_{\text{off}}$ and $\mathbf{A}_{\text{on}}$

In order to prove the closed-form expression of the determinant of (47) in Theorem 4, we will exploit the following lemma that presents a formula for the determinant of a block matrix.

Lemma 2 *Let a square matrix* $\mathbf{M}$ *be defined by blocks:*

$$\mathbf{M} = \begin{pmatrix} \mathbf{M^{11}} & \mathbf{M^{12}} \\ \mathbf{M^{21}} & \mathbf{M^{22}} \end{pmatrix},$$

Provided the existence of $\left(\mathbf{M^{22}}\right)^{-1}$*, the determinant of* $\mathbf{M}$ *is given by*

$$\det\left(\mathbf{M}\right) = \det\left(\mathbf{M^{22}}\right) \det\left(\mathbf{M^{11}} - \frac{1}{\det\left(\mathbf{M^{22}}\right)} \mathbf{M^{12}} \mathrm{Adj}^T\left(\mathbf{M^{22}}\right) \mathbf{M^{21}}\right),$$

where $\mathrm{Adj}^T\left(\mathbf{X}\right)$ *denotes the transpose of the Adjugate or Adjoint matrix of* $\mathbf{X}$*.*

We will also avail of the following theorem, which shows how to compute the determinant of a sum of matrices.

Lemma 3 (Matrix Determinant Lemma) *Let* $\mathbf{A}$ *be a non-singular square matrix and* $\mathbf{x}$*,* $\mathbf{y}$ *be column vectors of the dimension of* $\mathbf{A}$*, then*

$$\det\left(\mathbf{A} + \mathbf{x}\mathbf{y}^{\mathbf{T}}\right) = \det(\mathbf{A}) + \mathbf{y}^{\mathbf{T}} \mathrm{Adj}^T\left(\mathbf{A}\right) \mathbf{x}.$$

The proof of the previous lemmas can be found in [5], for example. Now, we use these theorems to prove the forthcoming lemma.

Lemma 4 *The determinant of* (47) *is given by*

1. ***Off Steady State***

$$\det\left(\mathbf{A}_{\mathrm{off}}\right) = \prod_{i=1}^{p} k_2^i k_{3f}^i - \prod_{i=1}^{p} k_1^i k_{3b}^i$$

2. ***On Steady State***

$$\det\left(\mathbf{A}_{\mathrm{on}}\right) = \prod_{i=1}^{p} k_1^i k_{3b}^i - \prod_{i=1}^{p} k_2^i k_{3f}^i$$

Proof The strategy of the proof follows a recursive application of the Lemma 2, finalised by the application of Lemma 3 to obtain a closed-form expression for the determinant. We note that applying $p-1$ times Lemma 2, the determinant of (47) can be expressed as

$$\det\left(\mathbf{A}\right) = \prod_{i=2}^{p} \det\left(\mathbf{A}^{ii}\right) \det\left(\mathbf{A}^{1\,1} - \prod_{i=2}^{p} \frac{1}{\det\left(\mathbf{A}^{ii}\right)} \left[\prod_{i=1}^{p-1} -\mathbf{A}^{i,i+1} \mathrm{Adj}^T\left(\mathbf{A}^{i+1,i+1}\right)\right] \mathbf{A}^{p1}\right). \tag{78}$$

Moreover, we note that

$$\begin{aligned} -\mathbf{A}^{p-1\,p} \mathrm{Adj}^T\left(\mathbf{A}^{pp}\right) \mathbf{A}^{p1} &= -\sigma^{p-1} \begin{pmatrix} 0 & -1 \\ 0 & 1 \end{pmatrix} \begin{pmatrix} -k_2^p & 0 \\ k_1^p \bar{c}_2^1 & -\mu^p \end{pmatrix} \sigma^p \begin{pmatrix} 0 & -1 \\ 0 & 1 \end{pmatrix} \\ &= k_{3f}^p \sigma^{p-1} \sigma^p \begin{pmatrix} 0 & -1 \\ 0 & 1 \end{pmatrix}. \end{aligned}$$

Where σ^i and μ^i have been defined in (50). Hence

$$\left[\prod_{i=1}^{p-1} -\mathbf{A}^{i,i+1}\mathrm{Adj}^T\left(\mathbf{A}^{i+1,i+1}\right)\right]\mathbf{A}^{p1} = \sigma^1\left[\prod_{i=2}^{p} k_{3f}^i\sigma^i\right]\begin{pmatrix}0 & -1\\ 0 & 1\end{pmatrix}.$$

Substituting the expression above into (78), yields

$$\det\left(\mathbf{A}\right) = \prod_{i=2}^{p}\det\left(\mathbf{A}^{ii}\right)\det\left(\mathbf{A}^{11} + \sigma^1\prod_{i=2}^{p}\frac{1}{\det\left(\mathbf{A}^{ii}\right)}\left[\prod_{i=2}^{p}k_{3f}^i\sigma^i\right]\begin{pmatrix}0 & -1\\ 0 & 1\end{pmatrix}\right).$$

By Lemma 3 and $\mathbf{A}^{ii}$ in (49a), the expression above becomes

$$\begin{aligned}\det\left(\mathbf{A}\right) &= \prod_{i=2}^{p}\det\left(\mathbf{A}^{ii}\right)\left[\det\left(\mathbf{A}^{11}\right) - \prod_{i=2}^{p}\frac{1}{\det\left(\mathbf{A}^{ii}\right)}\prod_{i=1}^{p}k_{3f}^i\sigma^i\right],\\ \det\left(\mathbf{A}\right) &= \prod_{i=1}^{p}k_2^i\mu^i - \prod_{i=1}^{p}k_{3f}^i\sigma^i. \end{aligned} \tag{79}$$

We further consider the definition of the steady states, to conclude the proof.

1. **Off Steady State**
   By substituting the definition of this equilibrium point in (35a), into (79), we obtain the expression

   $$\det\left(\mathbf{A}_{\mathrm{off}}\right) = \prod_{i=1}^{p}k_2^ik_{3f}^i - \prod_{i=1}^{p}k_1^ik_{3b}^i,$$

   as desired.
2. **On Steady State**
   This equilibrium point is parametrised by ϑ^{i+1}, defined in (36), via the relationships (39a) and (39b). Firstly, we analyse the product of the main blocks determinants in (79). By means of (39b) we can rewrite it as

   $$\begin{aligned}\det\left(\mathbf{A}_{\mathrm{on}}^{ii}\right) &= k_2^i\frac{k_{3f}^ik_2^{i+1}\mathrm{d}\left(\vartheta^{i+1}\right) - k_1^i\mathrm{n}\left(\vartheta^{i+1}\right)}{k_2^{i+1}\mathrm{d}\left(\vartheta^{i+1}\right)}\\ \det\left(\mathbf{A}_{\mathrm{on}}^{ii}\right) &= \mathrm{d}\left(\alpha^i\right)\frac{k_2^i\mathrm{d}\left(\vartheta^i\right)}{k_2^{i+1}\mathrm{d}\left(\vartheta^{i+1}\right)},\end{aligned}$$

   where we availed of the expression in (74). From the expression above, we note

   $$\begin{aligned}\prod_{i=1}^{p}\det\left(\mathbf{A}_{\mathrm{on}}^{ii}\right) &= \prod_{i=1}^{p}\mathrm{d}\left(\alpha^i\right)\frac{k_2^i\mathrm{d}\left(\vartheta^i\right)}{k_2^{i+1}\mathrm{d}\left(\vartheta^{i+1}\right)}\\ \prod_{i=1}^{p}\det\left(\mathbf{A}_{\mathrm{on}}^{ii}\right) &= \prod_{i=1}^{p}k_1^ik_{3b}^i.\end{aligned} \tag{80}$$

Secondly, we note that, with the expressions (38a) and (39b), $\bar{c}_1^i$ may be rewritten as

$$\bar{c}_1^i = \frac{k_2^{i+1} \mathrm{d}\left(\vartheta^{i+1}\right)}{k_1^i \mathrm{d}\left(\vartheta^i\right)}.$$

Hence the later product in (79) becomes

$$\prod_{i=1}^{p} k_{3f}^i k_1^i \bar{c}_i^1 = \prod_{i=1}^{p} k_{3f}^i k_2^{i+1}.$$

Subtraction of (80) and the relationship above, yields

$$\det\left(\mathbf{A}_{\mathrm{on}}\right) = \prod_{i=1}^{p} k_1^i k_{3b}^i - \prod_{i=1}^{p} k_{3f}^i k_2^i,$$

when exploiting the modularity of the product with respect to p.

□

Now, we provide the proof of Theorem 5, which determines the stability of the *on steady state* under the conditions on the parameters described in (64).

9.4 Proof of Theorem 5

Proof Accounting for the conditions (64), the solution for Ω^* in (59) is positive and real, for the positive sign of the square root. Let us rewrite this solution as

$$\Omega^* = -\left(k_{3f}^i\right)^2 + \sqrt{\left[\left(k_{3f}^i\right)^2 - \left(k_2^i\right)^2\right]\left[\left(k_{3f}^i\right)^2 - \left(\mu_{\mathrm{on}}^i\right)^2\right]} =: -\left(k_{3f}^i\right)^2 + \phi^i \eta^i, \tag{81}$$

where

$$\phi^i = \sqrt{\left(k_2^i\right)^2 - \left(k_{3f}^i\right)^2}, \tag{82a}$$

$$\eta^i = \sqrt{\left(\mu_{\mathrm{on}}^i\right)^2 - \left(k_{3f}^i\right)^2}. \tag{82b}$$

Then, from (58), the gain of the system evaluated in the peak frequency (81) is

$$\begin{aligned}
\gamma_{\text{on}}^i &= \sigma^i \sqrt{\frac{\phi^i\eta^i}{\left[-\left(k_{3f}^i\right)^2+\phi^i\eta^i+(\mu_{\text{on}}^i)^2\right]\left[-\left(k_{3f}^i\right)^2+\phi^i\eta^i+\left(k_2^i\right)^2\right]}} \\
&= \sigma^i \sqrt{\frac{1}{(\phi^i)^2+2\phi^i\eta^i+(\eta^i)^2}} \\
&= \frac{\sigma^i}{\phi^i+\eta^i} \\
&= \frac{\sigma^i}{\sqrt{\left(k_2^i\right)^2-\left(k_{3f}^i\right)^2}+\sqrt{(\mu_{\text{on}}^i)^2-\left(k_{3f}^i\right)^2}} \\
&= \frac{\sigma^i k_{3f}^i}{\mu_{\text{on}}^i k_2^i}\frac{k_2^i}{k_{3f}^i}\frac{\mu_{\text{on}}^i}{\sqrt{\left(k_2^i\right)^2-\left(k_{3f}^i\right)^2}+\sqrt{(\mu_{\text{on}}^i)^2-\left(k_{3f}^i\right)^2}} \\
\gamma_{\text{on}}^i &= \frac{k_2^{i+1}k_{3f}^i}{k_1^i k_{3b}^i}\frac{k_2^{i+1}}{k_2^i}\left[\frac{\mathrm{d}\left(\vartheta^{i+1}\right)}{\mathrm{d}\left(\vartheta^i\right)}\right]^2 \frac{1}{\frac{k_{3f}^i}{\mu_{\text{on}}^i}\sqrt{1-\left(\frac{k_{3f}^i}{k_2^i}\right)^2}+\frac{k_{3f}^i}{k_2^i}\sqrt{1-\left(\frac{k_{3f}^i}{\mu_{\text{on}}^i}\right)^2}}.
\end{aligned} \tag{83}$$

In the derivation of the expression above, we exploited the definitions in (82) and (50). Except for the last factor, the expression above resembles the gain for the *on steady state* in (77), analysed in Theorem 4. Moreover, we have just considered that for *some* i, the conditions in (64) are satisfied. Then the stability condition form the Small Gain Theorem can be expressed as

$$\begin{aligned}
\prod_{i=1}^{p}\frac{k_2^{i+1}k_{3f}^i}{k_1^i k_{3b}^i}\left(\theta^i\right)^{-1} &< 1 \\
\prod_{i=1}^{p}\frac{k_2^{i+1}k_{3f}^i}{k_1^i k_{3b}^i} &< \prod_{i=1}^{p}\theta^i,
\end{aligned}$$

where the definition of θ^i is given in (66). Although exact, the condition above might be an intricate function of the parameters. In the following, we pursue a tractable bound of γ_{on}^i. To this end we note that (64c) implies

$$\begin{aligned}
1-\left(\frac{k_{3f}^i}{k_2^i}\right)^2 &> \left(\frac{k_{3f}^i}{\mu_{\text{on}}^i}\right)^2 \\
1-\left(\frac{k_{3f}^i}{\mu_{\text{on}}^i}\right)^2 &> \left(\frac{k_{3f}^i}{k_2^i}\right)^2
\end{aligned}$$

Using these two last inequalities in (83), we obtain the bound

$$\begin{aligned}
\gamma_{\text{on}}^i &< \frac{\sigma^i}{k_2^i \frac{k_{3f}^i}{\mu_{\text{on}}^i} + \mu_{\text{on}}^i \frac{k_{3f}^i}{k_2^i}} \\
&= \frac{k_2^i}{k_{3f}^i} \frac{\sigma^i \mu_{\text{on}}^i}{\left(k_2^i\right)^2 + \left(\mu_{\text{on}}^i\right)^2} \\
&= \frac{\sigma^i k_{3f}^i}{\mu_{\text{on}}^i k_2^i} \left(\frac{k_2^i}{k_{3f}^i}\right)^2 \frac{\left(\mu_{\text{on}}^i\right)^2}{\left(k_2^i\right)^2 + \left(\mu_{\text{on}}^i\right)^2} \\
&= \frac{k_2^{i+1} k_{3f}^i}{k_1^i k_{3b}^i} \frac{k_2^{i+1}}{k_2^i} \left[\frac{\mathrm{d}\left(\vartheta^{i+1}\right)}{\mathrm{d}\left(\vartheta^i\right)}\right]^2 \left(\frac{k_2^i}{k_{3f}^i}\right)^2 \frac{\left(\mu_{\text{on}}^i\right)^2}{\left(k_2^i\right)^2 + \left(\mu_{\text{on}}^i\right)^2} \\
&< \frac{k_2^{i+1} k_{3f}^i}{k_1^i k_{3b}^i} \frac{k_2^{i+1}}{k_2^i} \left[\frac{\mathrm{d}\left(\vartheta^{i+1}\right)}{\mathrm{d}\left(\vartheta^i\right)}\right]^2 \left(\frac{k_2^i}{k_{3f}^i}\right)^2 .
\end{aligned}$$

Here we used the definitions of μ_{on}^i and σ^i in (50). Again, the expression above resembles the gain for the *on steady state* in (77), analysed in Theorem 4. Since the conditions in (64) just hold for some i, the stability of the closed loop is guaranteed if (67) holds. □

References

1. Albeck, J.G., Burke, J.M., Spencer, S.L., Lauffenburger, D.A., Sorger, P.K.: Modeling a snap-action, variable-delay switch controlling extrinsic cell death. PLoS Biol **6**(12), e299 (2008). DOI 10.1371/journal.pbio.0060299
2. Alon, U.: An introduction to systems biology: design principles of biological circuits, vol. 10. CRC press (2007)
3. Arcak, M., Sontag, E.D.: Diagonal stability of a class of cyclic systems and its connection with the secant criterion. Automatica **42**, 1531–1537 (2006)
4. Bentele, M., Lavrik, I., Ulrich, M., Stosser, S., Heermann, D.W., Kalthoff, H., Krammer, P.H., Eils, R.: Mathematical modeling reveals threshold mechanism in CD95-induced apoptosis. The Journal of Cell Biology **166**(6), 839–851 (2004). DOI 10.1083/jcb.200404158
5. Bernstein, D.S.: Matrix mathematics: theory, facts, and formulas 2nd Ed. Princeton University Press (2009)
6. Brandman, O., Meyer, T.: Feedback loops shape cellular signals in space and time. Science **322**(5900), 390–395 (2008). DOI 10.1126/science.1160617
7. Cowling, V., Downward, J.: Caspase-6 is the direct activator of caspase-8 in the cytochrome c-induced apoptosis pathway: absolute requirement for removal of caspase-6 prodomain. Cell Death and Differentiation **9**(10), 1046–1056 (2002). DOI 10.1038/sj.cdd.4401065
8. Craciun, G., Helton, J.W., Williams, R.J.: Homotopy methods for counting reaction network equilibria. Mathematical Biosciences **216**(2), 140 – 149 (2008). DOI 10.1016/j.mbs.2008.09.001
9. Du, C., Fang, M., Li, Y., Li, L., Wang, X.: Smac, a mitochondrial protein that promotes cytochrome c-dependent caspase activation by eliminating IAP inhibition. Cell **102**(1), 33–42 (2000). PMID: 10929711
10. Eissing, T., Conzelmann, H., Gilles, E.D., Allgower, F., Bullinger, E., Scheurich, P.: Bistability Analyses of a Caspase Activation Model for Receptor-induced Apoptosis. J. Biol. Chem. **279**(35), 36,892–36,897 (2004). DOI 10.1074/jbc.M404893200

11. Feinberg, M.: The existence and uniqueness of steady states for a class of chemical reaction networks. Archive for Rational Mechanics and Analysis **132**, 311–370 (1995). 10.1007/BF00375614
12. Ferrell James E, J.: Self-perpetuating states in signal transduction: positive feedback, double-negative feedback and bistability. Current Opinion in Cell Biology **14**(2), 140–148 (2002). PMID: 11891111
13. Graham, R.K., Ehrnhoefer, D.E., Hayden, M.R.: Caspase-6 and neurodegeneration. Trends in Neurosciences **34**(12), 646–656 (2011). DOI 10.1016/j.tins.2011.09.001
14. Green, D.R., Kroemer, G.: The pathophysiology of mitochondrial cell death. Science **305**(5684), 626–629 (2004). DOI 10.1126/science.1099320
15. Hori, Y., Kim, T.H., Hara, S.: Existence criteria of periodic oscillations in cyclic gene regulatory networks. Automatica **47**(6), 1203 – 1209 (2011). DOI 10.1016/j.automatica.2011.02.042. Special Issue on Systems Biology
16. Huber, H.J., Duessmann, H., Wenus, J., Kilbride, S.M., Prehn, J.H.: Mathematical modelling of the mitochondrial apoptosis pathway. Biochimica et Biophysica Acta (BBA) - Molecular Cell Research **1813**(4), 608–615 (2011). DOI 10.1016/j.bbamcr.2010.10.004
17. Huber, H.J., Laussmann, M.A., Prehn, J.H., Rehm, M.: Diffusion is capable of translating anisotropic apoptosis initiation into a homogeneous execution of cell death. BMC Systems Biology **4**(9) (2010). DOI 10.1186/1752-0509-4-9
18. Inoue, S., Browne, G., Melino, G., Cohen, G.M.: Ordering of caspases in cells undergoing apoptosis by the intrinsic pathway. Cell Death & Differentiation **16**(7), 1053–1061 (2009). DOI 10.1038/cdd.2009.29
19. Jovanovic, M., Arcak, M., Sontag, E.: A passivity-based approach to stability of spatially distributed systems with a cyclic interconnection structure. Automatic Control, IEEE Transactions on **53**(Special Issue), 75 –86 (2008). DOI 10.1109/TAC.2007.911318
20. Kappelhoff, J., Liu, S., Dugdale, M., Dymianiw, D., Linton, L., Huber, R.: Practical considerations when using temperature to obtain rate constants and activation thermodynamics of enzymes with two catalytic steps: Native and N460T-β-Galactosidase *E. coli* as examples. The Protein Journal **28**(2), 96–103 (2009). DOI 10.1007/s10930-009-9168-1
21. Khalil, H.K.: Nonlinear Systems (3rd Edition). Prentice Hall (2001)
22. Kuranaga, E.: Caspase signaling in animal development. Development, Growth and Differentiation **53**(2), 137–148 (2011). DOI 10.1111/j.1440-169X.2010.01237.x
23. Legewie, S., Blüthgen, N., Herzel, H.: Mathematical Modeling Identifies Inhibitors of Apoptosis as Mediators of Positive Feedback and Bistability. PLoS Computational Biology **2**(9), e120+ (2006). DOI 10.1371/journal.pcbi.0020120
24. López-Caamal, F., García, M.R., Middleton, R.H., Huber, H.J.: Positive feedback in the Akt/mTOR pathway and its implications for growth signal progression in skeletal muscle cells: An analytical study. Journal of Theoretical Biology **301**(0), 15–27 (2012). DOI 10.1016/j.jtbi.2012.01.026
25. Martnez-Antonio, A., Janga, S.C., Thieffry, D.: Functional organisation of escherichia coli transcriptional regulatory network. Journal of Molecular Biology **381**(1), 238–247 (2008). DOI 10.1016/j.jmb.2008.05.054
26. Nikolaev, A., McLaughlin, T., O'Leary, D.D., Tessier-Lavigne, M.: APP binds DR6 to trigger axon pruning and neuron death via distinct caspases. Nature **457**(7232), 981–989 (2009). DOI 10.1038/nature07767
27. O'Connor, C.L., Anguissola, S., Huber, H.J., Dussmann, H., Prehn, J.H., Rehm, M.: Intracellular signaling dynamics during apoptosis execution in the presence or absence of x-linked-inhibitor-of-apoptosis-protein. Biochimica et Biophysica Acta (BBA) - Molecular Cell Research **1783**(10), 1903–1913 (2008). DOI 10.1016/j.bbamcr.2008.05.025
28. Ogata, K.: Modern Control Engineering, 4th edn. Prentice Hall PTR, Upper Saddle River, NJ, USA (2001)
29. Rehm, M., Huber, H., Dussmann, H., Prehn, J.: Systems analysis of effector caspase activation and its control by x-linked inhibitor of apoptosis protein. EMBO (2006)
30. Skogestad, S., Postlethwaite, I.: Multivariable Feedback Control: Analysis and Design. John Wiley & Sons (2005)

31. Slee, E.A., Keogh, S.A., Martin, S.J.: Cleavage of BID during cytotoxic drug and UV radiation-induced apoptosis occurs downstream of the point of bcl-2 action and is catalysed by caspase-3: a potential feedback loop for amplification of apoptosis-associated mitochondrial cytochrome c release. Cell Death and Differentiation **7**(6), 556–565 (2000). DOI 10.1038/sj.cdd.4400689
32. Strogatz, S.H.: Nonlinear Dynamics And Chaos: With Applications To Physics, Biology, Chemistry, And Engineering (Studies in Nonlinearity), 1 edn. Studies in nonlinearity. Perseus Books Group (1994)
33. Turing, A.M.: The Chemical Basis of Morphogenesis. Philosophical Transactions of the Royal Society of London. Series B, Biological Sciences **237**(641), 37–72 (1952)
34. Williams, D.W., Kondo, S., Krzyzanowska, A., Hiromi, Y., Truman, J.W.: Local caspase activity directs engulfment of dendrites during pruning. Nature Neuroscience **9**(10), 1234–1236 (2006). DOI 10.1038/nn1774
35. Würstle, M.L., Laussmann, M.A., Rehm, M.: The caspase-8 dimerization/dissociation balance is a highly potent regulator of caspase-8, -3, -6 signaling. Journal of Biological Chemistry **285**(43), 33,209–33,218 (2010). DOI 10.1074/jbc.M110.113860
36. Zou, H., Yang, R., Hao, J., Wang, J., Sun, C., Fesik, S.W., Wu, J.C., Tomaselli, K.J., Armstrong, R.C.: Regulation of the apaf-1/caspase-9 apoptosome by caspase-3 and XIAP. The Journal of biological chemistry **278**(10), 8091–8098 (2003). DOI 10.1074/jbc.M204783200. PMID: 12506111

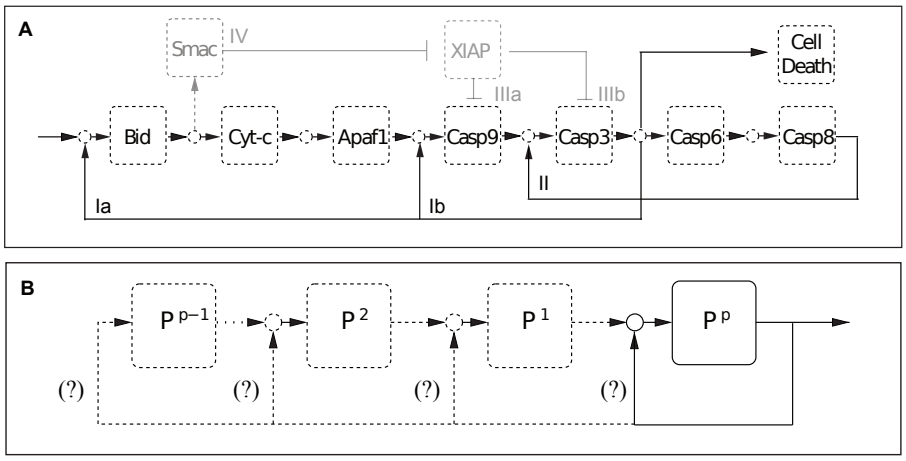

Fig. 1 Feedback loop of variable length as an abstraction of typical regulation patterns in signal transduction. **A** Feedback cycles in intrinsic apoptosis. Proteolytic cleavage of the BH3-only protein BID initiates a cycle of proteolytic events culminating in the activation of caspase-3 which executes cell death by cleaving DNA and cytoskeleton. **I** Once activated, caspase-3 further activates BID (Ia) and Caspase-9 (Ib), establishing a positive feedback loop. **II** Positive feedback downstream of caspase-3 trough initiation of a caspase-3/6/8 cascade as studied in the text. **III-IV** While the anti-apoptotic protein XIAP may attenuate caspase-3 (IIIa) and -9 (IIIb) activity and itself may be attenuated by the pro-apototic proteins SMAC, this pathway is not present in cells with XIAP-deficiency [27]. **B** The p-tier feedback loop as studied in the manuscript. Boxes indicate protein species. Active and inactive protein forms, protein production and degradation are not explicitly specified. Arrows indicate protein activation, whereas circles indicate signal summation. The steady states and their stability dependent on chain length are investigated.

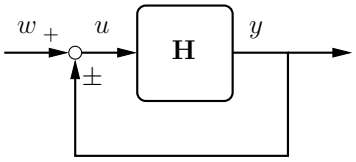

Fig. 2 Unity feedback connection of a system $\mathbf{H}(s)$. Theorem 2 establishes conditions under which the closed-loop system is stable, provided $\mathbf{H}(s)$ is stable.

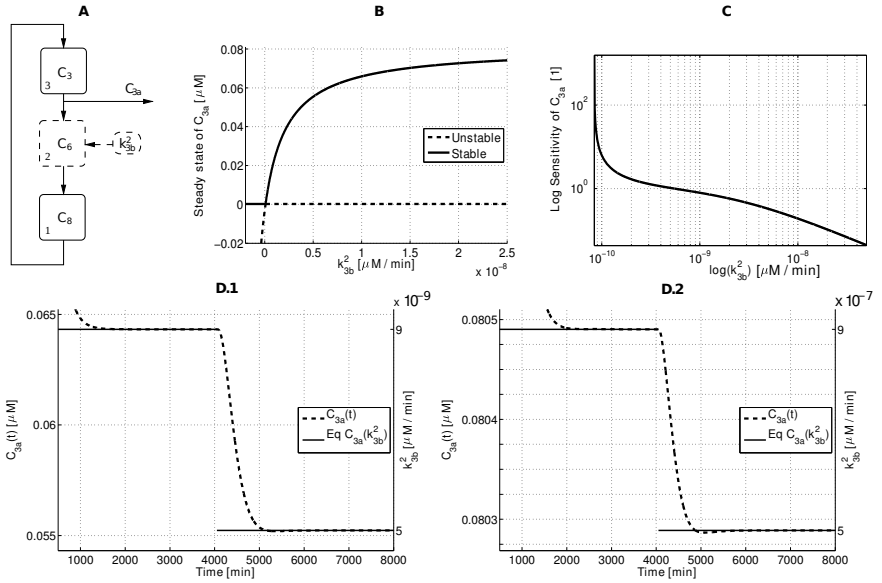

Fig. 3 Dynamical response of active caspase-3 (C_{3a}) under variation of the synthesis of caspase-6 (k^2_{3b}). The rest of the parameters were taken from the supplemental material of [35]. In panel **A** caspase-6 (C_6) activates caspase-8 (C_8), which further activates caspase-3 (C_3); to complete the loop, caspase-3 activates caspase-6. The detailed mechanism of activation for all panels is described in (31). The sequence of activation (superindex i in (31)) is represented by the number adjacent to each box. Panel **B** shows the equilibrium points for active caspase-3 as a function of the synthesis rate of caspase-6 $\left(k^2_{3b}\right)$ as presented in (69). The solid line represent locally stable equilibrium points, whereas the dashed line depicts unstable equilibrium points. In turn, panel **C** shows the logarithmic sensitivity of C_{3a} with respect to $\log\left(k^2_{3b}\right)$, as expressed in (71). Finally, the lower panels **D** show concentration over time of C_{3a} in response to a sudden variation of k^2_{3b}. The dashed line depicts the concentration of C_{3a} as a function of time, whereas the solid line shows the equilibrium point as a function of k^2_{3b}. Despite the absolute variation of the parameter k^2_{3b} was lower in **D.1** than in **D.2**, the effect of this variation was much higher in the corresponding activation of caspase-3. (Please, note the different scales in the left and right vertical axes between **D.1** and **D.2**). As consequence, in certain ranges, a small variation of k^2_{3b} yields a severe effect on the location of the equilibrium point of C_{3a}, similar to a 'molecular transistor'. Hence, a fine tuning of the synthesis of inactive caspase-6 is crucial for pronounced activation of caspase-3.